

Inclusive decays of η_c and η_b at NNLO with large n_f resummation

Nora Brambilla,^{1,2,3} Hee Sok Chung,^{1,3} and Javad Komijani^{1,2,*}

¹*Physik-Department, Technische Universität München, James-Franck-Straße 1, 85748 Garching, Germany*

²*Institute for Advanced Study, Technische Universität München, Lichtenbergstraße 2 a, 85748 Garching, Germany*

³*Excellence Cluster Universe, Technische Universität München, Boltzmannstraße 2, D-85748, Garching, Germany*



(Received 5 October 2018; published 19 December 2018)

Based on the nonrelativistic QCD factorization theorem, we resum QCD corrections to the inclusive decay rate of η_c and η_b in the large- n_f limit using bubble chain resummation. By employing dimensional regularization, we show explicitly the cancellation of the infrared renormalon ambiguity in the factorization formula at leading order in v in the large- n_f limit, where v is the typical heavy quark velocity inside the meson. We also make predictions of the ratio of the inclusive decay rate to the decay rate into two photons. By comparing our results with a fixed-order calculation we conclude that resummation of QCD corrections is crucial in making an unambiguous prediction. We also find significant corrections beyond the large- n_f limit for the decay of η_c , which may imply that QCD corrections need to be resummed beyond the large- n_f limit to make an accurate prediction of the decay rate.

DOI: [10.1103/PhysRevD.98.114020](https://doi.org/10.1103/PhysRevD.98.114020)

I. INTRODUCTION

Nowadays there is much experimental effort devoted to investigating the nature of heavy quarkonium states. Precision measurements of the properties of heavy quarkonia such as their masses, decays or transitions can be done at future and ongoing experiments like Belle II, BESIII, and LHCb at CERN. A good understanding of the nature of heavy quarkonium states is essential in exploring other processes that involve heavy quarkonia such as their production in high energy collisions. Following the substantial success of the B factories [1], the Belle II experiment at KEK in Japan is going to collect 50 times more data of what Belle obtained and will be able to investigate the properties of pseudoscalar bottomonium η_b state and the corresponding charmonium η_c state.

One of the basic observables regarding heavy quarkonium is its inclusive decay rate. Theoretical predictions of the inclusive decay rate of η_c and η_b have long been pursued using nonrelativistic QCD (NRQCD), which is an effective theory providing a factorization formalism that

separates the perturbative short-distance contributions from the nonperturbative long-distance ones [2]. The NRQCD factorization formula for the decay rate of a heavy quarkonium is a sum over products of NRQCD long-distance matrix elements (LDMEs) and the corresponding short-distance coefficients (SDCs). The NRQCD power counting attributes to the LDMEs a specific scaling with v , where v is the relative velocity between the heavy quark and the heavy antiquark in the quarkonium. The SDCs may be computed in perturbation theory. Therefore, the sum in the NRQCD factorization formula is an expansion in powers of v and α_s .

There are two major obstacles in achieving theoretical predictions of the decay rates of η_c and η_b with high accuracy. First, even though the expressions for the SDCs that contribute to the decay rates are available through order v^7 (relative order v^4) [3,4],¹ the NRQCD LDMEs are generally not known very well beyond the one at leading order in v . Second, the perturbative corrections to the SDCs, which are currently known to next-to-next-to-leading order (NNLO) in the strong coupling constant α_s , are uncomfortably large, hinting at a possible failure of the convergence of the perturbation series. Especially, the nonconvergence of the perturbation series may correspond to renormalon ambiguities that arise when computing diagrams in dimensional regularization and resumming the perturbation series by using the Borel transform.

*Present address: School of Physics and Astronomy, University of Glasgow, Glasgow G12 8QQ, United Kingdom.

Published by the American Physical Society under the terms of the [Creative Commons Attribution 4.0 International license](https://creativecommons.org/licenses/by/4.0/). Further distribution of this work must maintain attribution to the author(s) and the published article's title, journal citation, and DOI. Funded by SCOAP³.

¹Here, we adopt the power counting rules in Ref. [2].

These difficulties can be partially overcome by considering R , the ratio of the inclusive decay rate to the electromagnetic decay rate to two photons. A considerable simplification occurs in R : not only it is independent of the leading-order LDME, but also the correction of relative order $\alpha_s^0 v^2$ cancels in R . The NRQCD factorization scale dependence, which arises in the corrections of relative order α_s^2 and $\alpha_s v^2$, also cancel in R . Finally, the renormalon ambiguities associated with the loop corrections to the initial heavy quark-antiquark states also cancel in the ratio up to relative order v^2 . Nevertheless, the renormalon ambiguities associated with the final-state gluons in the inclusive decay rate survive in R , so the perturbation series for R still suffers from nonconvergence.

In this paper, we consider the resummation of perturbative corrections to the ratio R that are associated with the chain of vacuum-polarization bubbles in the final-state gluons in the inclusive decay rate of η_Q , where $Q = c$ or b . In Ref. [5], the resummation has been performed by imposing an infrared cutoff in the calculation of perturbative QCD corrections, which allows one to avoid renormalon ambiguities that appear in the resummation if dimensional regularization is used instead. In this work, we employ dimensional regularization to compute corrections in perturbative QCD in the limit of large number of active quark flavors n_f and show explicitly in this limit the appearance of renormalon ambiguities in the perturbative QCD amplitude. We also show, by computing the perturbative corrections in NRQCD, that perturbative NRQCD reproduces exactly the large n_f leading renormalon ambiguity in perturbative QCD, and therefore, the NRQCD factorization formula is free of this kind of renormalon ambiguities. We argue that, due to the limited knowledge on NRQCD LDMEs of higher orders in v , using a hard cutoff instead of dimensional regularization to regularize the ultraviolet divergences in NRQCD leads to an expression for the decay rate of η_Q that is more useful for phenomenological applications. We also combine our resummed calculation with the perturbative calculation of R , which is currently known to NNLO in α_s and provide updated numerical results for both η_c and η_b .

The paper is organized as follows. In Sec. II we consider the resummation of vacuum-polarization bubble chains in the η_Q decay rate and obtain a resummed expression for R . We also combine the resummed result with the perturbative calculation of R . In Sec. III we present our numerical results for the ratio R and compare them to experimental data [6]. We conclude in Sec. IV.

II. RESUMMATION OF VACUUM-POLARIZATION BUBBLE CHAINS IN R

In this section, we present the SDCs that contribute to the inclusive decay rate of η_Q . To this end, we first shortly discuss the NRQCD factorization formula for the decay

rate of η_Q . Then we use the factorization formula to compute the decay rate of a perturbative $Q\bar{Q}$ state in perturbative QCD and perturbative NRQCD. Finally, the SDCs are obtained by comparing the expressions for the decay rate computed in QCD and NRQCD.

A. NRQCD factorization for the decay rate of η_Q

The NRQCD factorization formula for the decay rate of η_Q , valid through relative order v^3 , reads [3]

$$\begin{aligned} \Gamma_{\eta_Q} = & 2\text{Im} \left[\frac{f_1(^1S_0)}{m^2} \right] \langle \eta_Q | \mathcal{O}_1(^1S_0) | \eta_Q \rangle \\ & + 2\text{Im} \left[\frac{g_1(^1S_0)}{m^4} \right] \langle \eta_Q | \mathcal{P}_1(^1S_0) | \eta_Q \rangle \\ & + 2\text{Im} \left[\frac{f_8(^3S_1)}{m^2} \right] \langle \eta_Q | \mathcal{O}_8(^3S_1) | \eta_Q \rangle, \end{aligned} \quad (1)$$

where m is the pole mass of the heavy quark Q . The four-quark operators $\mathcal{O}_1(^1S_0)$, $\mathcal{P}_1(^1S_0)$ and $\mathcal{O}_8(^3S_1)$ are given by

$$\mathcal{O}_1(^1S_0) = \psi^\dagger \chi \chi^\dagger \psi, \quad (2a)$$

$$\mathcal{P}_1(^1S_0) = \frac{1}{2} \left[\psi^\dagger \chi \chi^\dagger \left(-\frac{i \overleftrightarrow{\mathbf{D}}}{2} \right)^2 \psi + \psi^\dagger \left(-\frac{i \overleftrightarrow{\mathbf{D}}}{2} \right)^2 \chi \chi^\dagger \psi \right], \quad (2b)$$

$$\mathcal{O}_8(^3S_1) = \psi^\dagger T^a \sigma^i \chi \chi^\dagger T^a \sigma^i \psi. \quad (2c)$$

Here, ψ and χ are the Pauli spinor field operators that annihilates a heavy quark and creates a heavy antiquark, respectively. The operator $\overleftrightarrow{\mathbf{D}}$ is the difference between the covariant derivative acting on the spinor to the right and on the spinor to the left, so that $\chi^\dagger \overleftrightarrow{\mathbf{D}} \psi = \chi^\dagger \mathbf{D} \psi - (\mathbf{D} \chi^\dagger) \psi$.

The LDMEs $\langle \eta_Q | \mathcal{O}_1(^1S_0) | \eta_Q \rangle$, $\langle \eta_Q | \mathcal{P}_1(^1S_0) | \eta_Q \rangle$, and $\langle \eta_Q | \mathcal{O}_8(^3S_1) | \eta_Q \rangle$ are nonperturbative quantities that correspond to the probabilities to find $Q\bar{Q}$ pairs in specific color and angular-momentum states in the η_Q state. According to the power counting of Ref. [2], $\langle \eta_Q | \mathcal{O}_1(^1S_0) | \eta_Q \rangle$, which scales like v^3 , is the LDME at leading order in v ; $\langle \eta_Q | \mathcal{P}_1(^1S_0) | \eta_Q \rangle$ is suppressed by v^2 compared to the leading-order LDME [the suppression comes from the two powers of derivatives in the operator $\mathcal{P}_1(^1S_0)$] and scales like v^5 ; $\langle \eta_Q | \mathcal{O}_8(^3S_1) | \eta_Q \rangle$, which scales like v^6 , is suppressed by v^3 compared to $\langle \eta_Q | \mathcal{O}_1(^1S_0) | \eta_Q \rangle$. The suppression of the LDME $\langle \eta_Q | \mathcal{O}_8(^3S_1) | \eta_Q \rangle$ occurs because the operator $\mathcal{O}_8(^3S_1)$ annihilates and creates $Q\bar{Q}$ in a color-octet state through a spin-flip process [2].

Power counting rules that are more conservative than those of Ref. [2] have been suggested in Refs. [7,8]. In that power counting, which assumes Λ_{QCD} to be larger than $m v^2$, the LDME $\langle \eta_Q | \mathcal{P}_1(^1S_0) | \eta_Q \rangle$ scales like before, i.e.,

like $m^2 v^5$, while $\langle \eta_Q | \mathcal{O}_8(^3S_1) | \eta_Q \rangle$ scales like $v^3 \Lambda_{\text{QCD}}^2 / m^2$. Moreover, there are two additional color-octet LDMEs that scale like $v^3 \Lambda_{\text{QCD}}^2 / m^2$ and $\Lambda_{\text{QCD}}^2 v^3$ respectively, which are given by $\langle \eta_Q | \mathcal{O}_8(^1S_0) | \eta_Q \rangle = \langle \eta_Q | \psi^\dagger T^a \chi \chi^\dagger T^a \psi | \eta_Q \rangle$ and $\langle \eta_Q | \mathcal{O}_8(^1P_1) | \eta_Q \rangle = \langle \eta_Q | \psi^\dagger (-\frac{i}{2} \overleftrightarrow{\mathbf{D}}) T^a \chi \cdot \chi^\dagger (-\frac{i}{2} \overleftrightarrow{\mathbf{D}}) T^a \psi | \eta_Q \rangle$. Therefore, if we adopt the power counting rules in Refs. [7,8], Eq. (1) should include the above matrix elements to be valid through relative order $\Lambda_{\text{QCD}}^2 / m^2$. Considering, however, that in our numerical results, we will ignore the contribution from the color-octet LDME $\langle \eta_Q | \mathcal{O}_8(^3S_1) | \eta_Q \rangle$ and account for its effect only in the uncertainties, and that the additional color-octet LDMEs ignored in Eq. (1) do not affect the calculation of the renormalon ambiguities that we consider in this paper, we conclude that we may consistently neglect also the additional color-octet LDMEs $\langle \eta_Q | \mathcal{O}_8(^1S_0) | \eta_Q \rangle$ and $\langle \eta_Q | \mathcal{O}_8(^1P_1) | \eta_Q \rangle$, whose effect is included in the uncertainties. This is equivalent to assuming $mv \gg \Lambda_{\text{QCD}}$ and restricting our calculation to a precision of relative order v^2 .

The imaginary parts of the SDCs $2\text{Im}[f_1(^1S_0)/m^2]$, $2\text{Im}[g_1(^1S_0)/m^4]$ and $2\text{Im}[f_8(^3S_1)/m^2]$ can be computed in perturbation theory. A general method to compute the SDCs is to consider Eq. (1) with the nonperturbative meson state replaced by the perturbative $Q\bar{Q}$ state with definite color and angular momentum,

$$\begin{aligned} \Gamma_{Q\bar{Q}(n)} &= 2\text{Im} \left[\frac{f_1(^1S_0)}{m^2} \right] \langle Q\bar{Q}(n) | \mathcal{O}_1(^1S_0) | Q\bar{Q}(n) \rangle \\ &+ 2\text{Im} \left[\frac{g_1(^1S_0)}{m^4} \right] \langle Q\bar{Q}(n) | \mathcal{P}_1(^1S_0) | Q\bar{Q}(n) \rangle \\ &+ 2\text{Im} \left[\frac{f_8(^3S_1)}{m^2} \right] \langle Q\bar{Q}(n) | \mathcal{O}_8(^3S_1) | Q\bar{Q}(n) \rangle. \end{aligned} \quad (3)$$

Here, n denotes the color and angular momentum state of the $Q\bar{Q}$. We can compute the $\Gamma_{Q\bar{Q}}$ on the left-hand side in perturbative QCD and compute the LDMEs on the right-hand side in perturbative NRQCD for the $Q\bar{Q}$ states in various color, spin and orbital angular momentum states. Then, the SDCs can be determined by comparing the expressions on the left- and right-hand sides. In fixed-order perturbation theory, all SDCs in Eq. (1) appear from order α_s^2 [2]. The SDC $2\text{Im}[f_1(^1S_0)/m^2]$ at leading order (LO) and next-to-leading order (NLO) in α_s has been computed in Refs. [9,10], and the corrections at next-to-next-to-leading order (NNLO) in α_s have been calculated recently in Ref. [11]. The SDC $2\text{Im}[g_1(^1S_0)/m^4]$ at LO in α_s has been computed in Ref. [12], and the corrections at NLO in α_s have been calculated in Ref. [13]. The SDC $2\text{Im}[f_8(^3S_1)/m^2]$ has been computed up to NLO accuracy in α_s in Ref. [14].

The analogous NRQCD factorization formula for the decay of η_Q into two photons, valid through relative order v^3 , reads²

$$\begin{aligned} \Gamma_{\eta_Q \rightarrow \gamma\gamma} &= 2\text{Im} \left[\frac{f_{\text{EM}}(^1S_0)}{m^2} \right] \langle \eta_Q | \mathcal{O}_{\text{EM}}(^1S_0) | \eta_Q \rangle \\ &+ 2\text{Im} \left[\frac{g_{\text{EM}}(^1S_0)}{m^4} \right] \langle \eta_Q | \mathcal{P}_{\text{EM}}(^1S_0) | \eta_Q \rangle, \end{aligned} \quad (4)$$

where the electromagnetic operators $\mathcal{O}_{\text{EM}}(^1S_0)$ and $\mathcal{P}_{\text{EM}}(^1S_0)$ are given by

$$\mathcal{O}_{\text{EM}}(^1S_0) = \psi^\dagger \chi |0\rangle \langle 0| \chi^\dagger \psi, \quad (5a)$$

$$\begin{aligned} \mathcal{P}_{\text{EM}}(^1S_0) &= \frac{1}{2} \left[\psi^\dagger \chi |0\rangle \langle 0| \chi^\dagger \left(-\frac{i}{2} \overleftrightarrow{\mathbf{D}} \right)^2 \psi \right. \\ &\left. + \psi^\dagger \left(-\frac{i}{2} \overleftrightarrow{\mathbf{D}} \right)^2 \chi |0\rangle \langle 0| \chi^\dagger \psi \right]. \end{aligned} \quad (5b)$$

Here, $|0\rangle$ is the QCD vacuum. The SDC $2\text{Im}[f_{\text{EM}}(^1S_0)/m^2]$ have been computed up to NNLO in α_s in fixed-order perturbation theory [9,15,16], and $2\text{Im}[g_{\text{EM}}(^1S_0)/m^4]$ is available up to NLO in α_s [12,13,17]. The electromagnetic LDMEs $\langle \eta_Q | \mathcal{O}_{\text{EM}}(^1S_0) | \eta_Q \rangle$ and $\langle \eta_Q | \mathcal{P}_{\text{EM}}(^1S_0) | \eta_Q \rangle$ can be related to the color-singlet LDMEs $\langle \eta_Q | \mathcal{O}_1(^1S_0) | \eta_Q \rangle$ and $\langle \eta_Q | \mathcal{P}_1(^1S_0) | \eta_Q \rangle$ by using the vacuum-saturation approximation, which holds up to corrections of relative order v^4 [2],

$$\langle \eta_Q | \mathcal{O}_{\text{EM}}(^1S_0) | \eta_Q \rangle = \langle \eta_Q | \mathcal{O}_1(^1S_0) | \eta_Q \rangle [1 + \mathcal{O}(v^4)], \quad (6a)$$

$$\langle \eta_Q | \mathcal{P}_{\text{EM}}(^1S_0) | \eta_Q \rangle = \langle \eta_Q | \mathcal{P}_1(^1S_0) | \eta_Q \rangle [1 + \mathcal{O}(v^4)]. \quad (6b)$$

Putting Eqs. (1) and (4) together, the NRQCD expression for the ratio R , valid up to relative order v^3 , is

$$\begin{aligned} R &= \frac{\text{Im}[f_1(^1S_0)/m^2]}{\text{Im}[f_{\text{EM}}(^1S_0)/m^2]} \left[1 + \left(\frac{\text{Im}[g_1(^1S_0)/m^4]}{\text{Im}[f_1(^1S_0)/m^2]} \right. \right. \\ &\left. \left. - \frac{\text{Im}[g_{\text{EM}}(^1S_0)/m^4]}{\text{Im}[f_{\text{EM}}(^1S_0)/m^2]} \right) \frac{\langle \eta_Q | \mathcal{P}_1(^1S_0) | \eta_Q \rangle}{\langle \eta_Q | \mathcal{O}_1(^1S_0) | \eta_Q \rangle} \right] \\ &+ \frac{\text{Im}[f_8(^3S_1)/m^2]}{\text{Im}[f_{\text{EM}}(^1S_0)/m^2]} \frac{\langle \eta_Q | \mathcal{O}_8(^3S_1) | \eta_Q \rangle}{\langle \eta_Q | \mathcal{O}_1(^1S_0) | \eta_Q \rangle}, \end{aligned} \quad (7)$$

where the second term in the square brackets corresponds to the correction at relative order v^2 , and the last term on the right-hand side gives the order- v^3 contribution. The order- v^2 correction to R vanishes at LO in α_s ; this is because the tree-level Feynman diagrams for $Q\bar{Q} \rightarrow gg$ and $Q\bar{Q} \rightarrow \gamma\gamma$ are same. The order- $\alpha_s v^2$ correction to R can be obtained

²This expression is also valid, up to relative orders v^2 and $\Lambda_{\text{QCD}}^2 / m^2$, in the more conservative power counting of Refs. [7,8].

from the order- $\alpha_s v^2$ corrections to Γ_{η_Q} and $\Gamma_{\eta_Q \rightarrow \gamma\gamma}$. The correction at order $\alpha_s v^2$ is numerically small for both η_c and η_b , and it is comparable to the nominal size of the order- v^3 correction, which is often neglected (and included in the uncertainties) because the color-octet matrix element $\langle \eta_Q | \mathcal{O}_8(^1S_0) | \eta_Q \rangle$ is not known. We will follow this approach also here when providing numerical results (see Sec. III), but we will keep the color-octet matrix element $\langle \eta_Q | \mathcal{O}_8(^1S_0) | \eta_Q \rangle$ when discussing the renormalon cancellation in the rest of this section.

It is known from fixed-order calculations that the NLO and NNLO corrections to the SDCs $\text{Im}[f_1(^1S_0)/m^2]$ and $\text{Im}[f_{\text{EM}}(^1S_0)/m^2]$ are large. Especially, there are large corrections that are associated with the running of α_s , where a factor of α_s is accompanied by a factor of the QCD beta function. One way to resum (partially) such corrections is to consider chains of vacuum-polarization bubbles, which reproduce fixed-order perturbation theory in the limit where the number of active quark flavors n_f is large [18–20]. In the ratio $\text{Im}[f_1(^1S_0)/m^2]/\text{Im}[f_{\text{EM}}(^1S_0)/m^2]$, the perturbative corrections at large n_f that arise from initial-state virtual gluons cancel [5]. Therefore, in R , it suffices to consider only the perturbative corrections to $\text{Im}[f_1(^1S_0)/m^2]$ at large n_f that arise from the final-state gluons. In the next part, we resum the QCD corrections to $2\text{Im}[f_1(^1S_0)/m^2]$ that are associated with the final-state gluons in the large n_f limit.

The series for QCD corrections corresponding to bubble-chain diagrams in general do not converge. If one attempts to make use of the Borel transform to carry out the resummation of such series, the nonconvergence manifests itself through singularities in the Borel plane. The inverse Borel transform becomes ill-defined when the singularities reside on the positive axis of the Borel plane. This gives rise to the so-called renormalon ambiguity in the resummed series. The origin of the problem is that loop integrals contain contributions from regions of small gluon momenta where perturbation theory breaks down (for QCD) [21]. In the factorization formula [Eq. (3)], loop integrals are partitioned so that contributions from small loop momenta are contained in the LDMEs. Therefore, the SDCs are free of infrared renormalon ambiguities if all possible LDMEs are included in the factorization formula. In practice, since we truncate the factorization formula at some orders in v , exact cancellations of renormalon ambiguities in the calculation of the SDCs through the matching will occur through the order in v at which the factorization formula is valid, and there will be remaining ambiguities that are suppressed by powers of v . We shall demonstrate the cancellation of leading renormalon ambiguities in the explicit calculation of $2\text{Im}[f_1(^1S_0)/m^2]$.

Following Ref. [5], we employ two methods to carry out the bubble-chain resummation. One method is naïve non-Abelianization (NNA), where we consider corrections to

the gluon propagator from n_f light quark loops, and we promote the light-quark part of the one-loop QCD beta function to the full one-loop QCD beta function $\beta_0 = (33/2 - n_f)/(6\pi)$ [22]. That is, we make the following replacement in the gluon propagator:

$$\frac{1}{k^2 + i\epsilon} \rightarrow K(x), \quad (8)$$

where $x \equiv k^2/(4m^2)$, $K(x) = \sum_{n=0}^{\infty} K^{(n)}(x)$ and

$$K^{(n)}(x) = \frac{(\alpha_s \beta_0)^n [d - \log(-x - i\epsilon)]^n}{4m^2(x + i\epsilon)}. \quad (9)$$

Here, d is given by

$$d = \log \frac{\mu^2}{4m^2} - C, \quad (10)$$

where, in the $\overline{\text{MS}}$ renormalization scheme, $C = -5/3$ and μ is the renormalization scale. The strong coupling constant α_s is also computed in the $\overline{\text{MS}}$ scheme at the scale μ . Another method is the background-field gauge (BFG) method, where the corrections to the gluon propagator from the gluon and the ghost loops that are gauge dependent are also taken into account [23]. In the BFG method in the R_ξ gauge, d is given by

$$d = \log \frac{\mu^2}{4m^2} + \frac{1}{\beta_0 \pi} \left[\frac{67}{12} - \frac{5}{18} n_f - \frac{3}{4} (\xi^2 - 1) - \frac{5}{3} - C \right], \quad (11)$$

where ξ is the gauge-fixing parameter. The choice $\xi = 1$ corresponds to the Feynman gauge. If we set $\xi^2 = 7/3$, we reproduce the NNA method. Hence, the NNA expression for the gluon propagator may be interpreted as a special case of the BFG expression for $\xi^2 = 7/3$. In order to examine the dependence on the gauge-fixing parameter ξ , we employ both the NNA method, which is equivalent to the BFG method for $\xi^2 = 7/3$, and the BFG method in the Feynman gauge ($\xi = 1$).

In the bubble-chain resummation, the left-hand side of Eq. (3) occurs from order α_s through the decay into a single bubble-chain gluon. In order to decay into a virtual gluon, the $Q\bar{Q}$ pair must be in a color-octet state. If we take the $Q\bar{Q}$ pair to be in the color-octet spin-triplet state and take the relative momentum between the Q and the \bar{Q} to vanish, the matrix element $\langle Q\bar{Q}_8(^3S_1) | \mathcal{O}_8(^3S_1) | Q\bar{Q}_8(^3S_1) \rangle$ occurs from order α_s^0 , and the matrix elements $\langle Q\bar{Q}_8(^3S_1) | \mathcal{O}_1(^1S_0) | Q\bar{Q}_8(^3S_1) \rangle$ and $\langle Q\bar{Q}_8(^3S_1) | \mathcal{P}_1(^1S_0) | Q\bar{Q}_8(^3S_1) \rangle$ vanish through order α_s^0 . Hence, the SDC $2\text{Im}[f_8(^3S_1)/m^2]$ occurs from order α_s , while the SDCs $2\text{Im}[f_1(^1S_0)/m^2]$ and $2\text{Im}[g_1(^1S_0)/m^4]$ vanish

through order α_s . The SDC $2\text{Im}[f_8(^3S_1)/m^2]$ has been computed in bubble-chain resummation in Ref. [5] as

$$2\text{Im}\left[\frac{f_8(^3S_1)}{m^2}\right] = -8\pi\alpha_s\text{Im}[K(1)]. \quad (12)$$

In order to compute the SDC $2\text{Im}[f_1(^1S_0)/m^2]$, we consider the left-hand side of Eq. (3) at order α_s^2 . At this order, $\Gamma_{Q\bar{Q}(n)}$ occurs through the decay into two bubble-chain gluons. If we take the $Q\bar{Q}$ pair to be in the color-singlet spin-singlet S -wave state, the matrix element $\langle Q\bar{Q}_1(^1S_0)|\mathcal{O}_1(^1S_0)|Q\bar{Q}_1(^1S_0)\rangle$ occurs from order α_s^0 , while the matrix element $\langle Q\bar{Q}_1(^1S_0)|\mathcal{O}_8(^3S_1)|Q\bar{Q}_1(^1S_0)\rangle$ occurs from order α_s . If we take the relative momentum q between the Q and the \bar{Q} to be zero, the matrix element $\langle Q\bar{Q}_1(^1S_0)|\mathcal{P}_1(^1S_0)|Q\bar{Q}_1(^1S_0)\rangle$ vanishes through order α_s^0 . Since the SDCs $2\text{Im}[f_1(^1S_0)/m^2]$ and $2\text{Im}[g_1(^1S_0)/m^4]$ appear from order α_s^2 , while the SDC $2\text{Im}[f_8(^3S_1)/m^2]$ occurs from order α_s , the contribution from the LDME $\langle Q\bar{Q}_1(^1S_0)|\mathcal{P}_1(^1S_0)|Q\bar{Q}_1(^1S_0)\rangle$ to the right-hand side of Eq. (3) vanishes at order α_s^2 when $q = 0$. This implies that if we take the $Q\bar{Q}$ state to be in the color-singlet 1S_0 state with $q = 0$, the SDC $2\text{Im}[g_1(^1S_0)/m^4]$ does not appear from the right-hand side of Eq. (3) at order α_s^2 , and the right-hand side of Eq. (3) involves at order α_s^2 the SDCs $2\text{Im}[f_1(^1S_0)/m^2]$ and $2\text{Im}[f_8(^3S_1)/m^2]$. Then, we can determine the SDC $2\text{Im}[f_1(^1S_0)/m^2]$ by comparing $\Gamma_{Q\bar{Q}_1(^1S_0)}$ [left-hand side of Eq. (3)] with the right-hand side of Eq. (3), where the LDMEs $\langle Q\bar{Q}_1(^1S_0)|\mathcal{O}_1(^1S_0)|Q\bar{Q}_1(^1S_0)\rangle$ and $\langle Q\bar{Q}_1(^1S_0)|\mathcal{O}_8(^3S_1)|Q\bar{Q}_1(^1S_0)\rangle$ are computed in perturbation theory. The SDC $2\text{Im}[f_1(^1S_0)/m^2]$ has been computed in bubble-chain resummation in Ref. [5] by regulating the infrared divergences using a hard infrared cutoff on the virtuality of the final-state gluons. While using such an infrared cutoff effectively removes renormalon ambiguities in $2\text{Im}[f_1(^1S_0)/m^2]$ by excluding contributions from arbitrarily soft gluon momenta, the cancellation of the renormalon ambiguities in the factorization formula becomes obscure.

The appearance of the renormalon ambiguity in $\Gamma_{Q\bar{Q}(n)}$ and the cancellation of the ambiguity in the SDC $2\text{Im}[f_1(^1S_0)/m^2]$ can be seen explicitly by computing

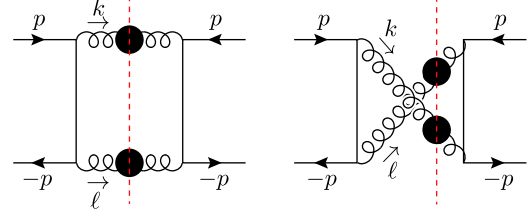


FIG. 1. Feynman diagrams that contribute to $\Gamma_{Q\bar{Q}_1(^1S_0)}$ at leading order in α_s in perturbative QCD. Curly lines with filled circles represent bubble-chain gluons and the dashed lines represent final-state cuts.

the SDC in dimensional regularization. In this section, we compute the SDC $2\text{Im}[f_1(^1S_0)/m^2]$ using bubble-chain resummation, by considering Eq. (3) where the $Q\bar{Q}$ is in the color-singlet spin-singlet S -wave state with vanishing relative momentum between the Q and the \bar{Q} . We regulate the infrared divergence using dimensional regularization.

B. Computation in perturbative QCD

We compute the decay rate of a $Q\bar{Q}$ pair in the color-singlet 1S_0 state into two bubble-chain gluons. We use nonrelativistic normalization for the $Q\bar{Q}$ states. We set the momentum of the Q and the \bar{Q} to be p . To project the $Q\bar{Q}$ pair onto the color-singlet spin-singlet state, we replace the spinors by

$$u(p)\bar{v}(p) \rightarrow \Pi_1(p, p)\Lambda_1, \quad (13)$$

where $\Pi_1(p, p)$ and Λ_1 are the spin-singlet and color-singlet projectors, respectively [24,25],

$$\Pi_1(p, p) = -\frac{1}{2\sqrt{2}m}(\not{p} + m)\gamma_5, \quad (14a)$$

$$\Lambda_1 = \frac{\mathbf{1}}{\sqrt{N_c}}. \quad (14b)$$

Here, $\mathbf{1}$ is the $SU(N_c)$ unit matrix. A straightforward calculation of the diagrams in Fig. 1 gives

$$\begin{aligned} \Gamma_{Q\bar{Q}_1(^1S_0)} &= \frac{1}{2} \int \frac{d^4k}{(2\pi)^4} \theta(k_0) \int \frac{d^4\ell}{(2\pi)^4} \theta(\ell_0) (2\pi)^4 \delta^{(4)} \times (2p - k - \ell) 2\text{Im}[K(x)] 2\text{Im}[K(y)] \\ &\times \left| \text{tr} \left\{ \left[(-ig\gamma^\nu T^b) \frac{i}{\not{p} - \not{k} - m + i\epsilon} (-ig\gamma^\mu T^a) + (-ig\gamma^\mu T^a) \frac{i}{-\not{p} + \not{k} - m + i\epsilon} (-ig\gamma^\nu T^b) \right] \right. \right. \\ &\left. \left. \times \Pi_1(p, p) \Lambda_1 \right\} \right|^2, \end{aligned} \quad (15)$$

where k and ℓ are the momenta of the final-state gluons, $g = \sqrt{4\pi\alpha_s}$, $x \equiv k^2/(4m^2)$, $y \equiv \ell^2/(4m^2)$, and the trace is over the color and gamma matrices. Even though we employ dimensional regularization, it suffices to work in four dimensions because in the current calculation, we encounter no divergences that require regularization. Then,

$$\Gamma_{Q\bar{Q}_1(\prime S_0)} = \frac{C_F g^4}{2} \frac{d^4 k}{(2\pi)^4} \theta(k_0) \int \frac{d^4 \ell}{(2\pi)^4} \theta(\ell_0) (2\pi)^4 \delta^{(4)}(2p - k - \ell) 2\text{Im}[K(x)] 2\text{Im}[K(y)] \frac{16}{m^2} \frac{(k \cdot p)^2 - m^2 k^2}{(k^2 - 2k \cdot p + i\epsilon)^2}. \quad (16)$$

We change the integration variables k^0, ℓ^0 to x and y , so that from $x = (k_0^2 - \mathbf{k}^2)/(4m^2)$ and $y = (\ell_0^2 - \boldsymbol{\ell}^2)/(4m^2)$, we obtain $dk_0 = 2m^2 dx/k_0$ and $d\ell_0 = 2m^2 dy/\ell_0$. Using the three-momentum components of the delta function to eliminate the integral over $\boldsymbol{\ell}$, we replace $\boldsymbol{\ell}$ with \mathbf{k} , and we obtain

$$\begin{aligned} \Gamma_{Q\bar{Q}_1(\prime S_0)} &= m^4 \frac{C_F g^4}{2} \frac{1}{2} \int_0^1 \frac{dx}{\pi} \int_0^1 \frac{dy}{\pi} \int \frac{d^3 \mathbf{k}}{(2\pi)^3} \\ &\times 2\pi \delta(2m - k_0 - \ell_0) \frac{\theta(\ell_0) \theta(k_0)}{\ell_0 k_0} \\ &\times 2\text{Im}[K(x)] 2\text{Im}[K(y)] \frac{16}{m^2} \frac{(k \cdot p)^2 - m^2 k^2}{(k^2 - 2k \cdot p + i\epsilon)^2}. \end{aligned} \quad (17)$$

Here, $k_0 = \sqrt{4m^2 x + \mathbf{k}^2}$ and $\ell_0 = \sqrt{4m^2 y + \mathbf{k}^2}$. The lower limits of the integrals over x and y are set by the fact that the imaginary parts of $K(x)$ and $K(y)$ vanish for negative values of x and y , respectively. The upper limits of the integrals over x and y are set by the fact that the maximum invariant mass of a final-state particle is equal to the invariant mass of the $Q\bar{Q}$ in the initial state. Since we have chosen a root of the square root function such that $k_0 > 0$ and $\ell_0 > 0$, we can drop $\theta(k_0)$ and $\theta(\ell_0)$. The remaining delta function in Eq. (17) constrains \mathbf{k}^2 to be $m^2[1 - 2(x + y) + (x - y)^2]$ and $1 - \sqrt{x} - \sqrt{y} \geq 0$; we then obtain

$$\begin{aligned} \Gamma_{Q\bar{Q}_1(\prime S_0)} &= \frac{2\pi C_F \alpha_s^2}{m^2} \sum_{n_1=0}^{\infty} \sum_{n_2=0}^{\infty} \int_0^1 \frac{dx}{2\pi} \int_0^1 \frac{dy}{2\pi} \\ &\times 2\text{Im}[4m^2 K^{(n_1)}(x)] 2\text{Im}[4m^2 K^{(n_2)}(x)] \\ &\times f(x, y) \theta(1 - \sqrt{x} - \sqrt{y}), \end{aligned} \quad (18)$$

where

$$f(x, y) = \frac{[1 - 2(x + y) + (x - y)^2]^{3/2}}{(1 - x - y)^2}. \quad (19)$$

The sum over n_1 and n_2 corresponds to insertions of n_1 and n_2 vacuum polarization bubbles to the two final-state gluon lines. If we use the relation

$$\begin{aligned} &\sum_{n=0}^{\infty} \int_0^1 \frac{dx}{2\pi} \text{Im}[4m^2 K^{(n)}(x)] F(x, y) \\ &= \sum_{n=0}^{\infty} (\alpha_s \beta_0)^n \left(\frac{d}{dt}\right)^n e^{td} \int_0^1 \frac{dx}{2\pi} \text{Im}\left[\frac{x^{-t} e^{i\pi t}}{x + i\epsilon}\right] F(x, y)|_{t=0}, \end{aligned} \quad (20)$$

which is valid for a generic function $F(x, y)$, we obtain

$$\begin{aligned} \Gamma_{Q\bar{Q}_1(\prime S_0)} &= \frac{2\pi C_F \alpha_s^2}{m^2} \sum_{n_1=0}^{\infty} \sum_{n_2=0}^{\infty} (\alpha_s \beta_0)^{n_1+n_2} \left(\frac{d}{dt}\right)^{n_1} \left(\frac{d}{d\tau}\right)^{n_2} \\ &\times e^{d(t+\tau)} T(t, \tau)|_{t=\tau=0}, \end{aligned} \quad (21)$$

where

$$\begin{aligned} T(t, \tau) &= \frac{1}{\pi^2} \int_0^1 dx \int_0^1 dy \text{Im}\left[\frac{x^{-t} e^{i\pi t}}{x + i\epsilon}\right] \text{Im}\left[\frac{y^{-\tau} e^{i\pi \tau}}{y + i\epsilon}\right] \\ &\times f(x, y) \theta(1 - \sqrt{x} - \sqrt{y}). \end{aligned} \quad (22)$$

We compute $T(t, \tau)$ in the Appendix. The summation in Eq. (21) can be rewritten in integral form by using the Borel summation formula: the Borel sum of $\sum_{n=0}^{\infty} a_n x^n$ is given by the integral

$$\int_0^{\infty} \frac{dt}{x} e^{-t/x} \phi(t), \quad (23)$$

where $\phi(x) = \sum_{n=0}^{\infty} a_n x^n / n!$. Using this formula, we rewrite Eq. (21) as

$$\Gamma_{Q\bar{Q}_1(\prime S_0)} = \frac{2\pi C_F \alpha_s^2}{m^2} \frac{1}{(\alpha_s \beta_0)^2} \int_0^{\infty} dt \int_0^{\infty} d\tau e^{-w(t+\tau)} T(t, \tau), \quad (24)$$

where

$$w = \frac{1}{\alpha_s \beta_0} - d. \quad (25)$$

Note that w depends on the scale μ through dependence on $\alpha_s(\mu)$ and d . This dependence, however, cancels at the level of one-loop running of $\alpha_s(\mu)$. The prefactor $2\pi C_F \alpha_s^2 / m^2$ corresponds to $\Gamma_{Q\bar{Q}_1(\prime S_0)}$ at leading order in α_s in fixed-order perturbation theory.

The function $T(t, \tau)$ is regular for $0 \leq t < 1$ and $0 \leq \tau < 1$. For $t \geq 1$ and $\tau \geq 1$, there are singularities in $T(t, \tau)$ that make the value of the integral in Eq. (24) ambiguous. The singularities in $T(t, \tau)$ that occur for the smallest values of t or τ are at $t = 1$ or $\tau = 1$,

$$\lim_{t \rightarrow 1} (1 - t) T(t, \tau) = -\frac{3}{\pi} \sin(\pi \tau), \quad (26a)$$

$$\lim_{\tau \rightarrow 1} (1 - \tau) T(t, \tau) = -\frac{3}{\pi} \sin(\pi t); \quad (26b)$$

see Eqs. (A20) and (A21). These singularities give the leading renormalon ambiguities in $\Gamma_{Q\bar{Q}_1(^1S_0)}$.

One way to estimate the size of the leading renormalon ambiguity is to inspect the difference between the results for the integral over t and τ when the integration contour is above the renormalon singularity and below the renormalon singularity [21]. From the residue theorem, the estimated ambiguity in $\Gamma_{Q\bar{Q}_1(^1S_0)}$ that arises from the leading renormalon singularity in $T(t, \tau)$ is

$$\begin{aligned} \delta\Gamma_{Q\bar{Q}_1(^1S_0)} &\sim \left| 2 \times 2\pi i \times \frac{2\pi C_F \alpha_s^2}{m^2} \frac{1}{(\alpha_s \beta_0)^2} \right. \\ &\quad \times \left. \int_0^\infty dt e^{-w(1+t)} \frac{3}{\pi} \sin(\pi t) \right| \\ &= \frac{2\pi C_F \alpha_s^2}{m^2} \frac{12\pi}{1 - 2\alpha_s \beta_0 d + (\alpha_s \beta_0)^2 (\pi^2 + d^2)} e^{-w}. \end{aligned} \quad (27)$$

For the case of η_c , the numerically estimated size of the leading renormalon ambiguity is of relative order one compared to $\Gamma_{Q\bar{Q}_1(^1S_0)}$ at leading order in α_s in fixed-order perturbation theory. This implies that for η_c , the value of the perturbation series $\Gamma_{Q\bar{Q}_1(^1S_0)}$ has an ambiguity of order one. Even for the case of η_b , the estimated ambiguity can be of relative order 10^{-1} , which is comparable to the nominal size of the order- v^2 corrections to the decay rate. Therefore, in

order to make an accurate theoretical prediction of the η_Q decay rate, it is crucial to have a factorization formula where such ambiguities are absent.

The renormalon ambiguities that arise from the singularities in $T(t, \tau)$ are located at $t = t_0$ or $\tau = t_0$ with $t_0 = 1$ being the smallest and involves a factor $e^{-t_0 w}$. If we consider only the one-loop running of α_s , this factor can be written as

$$e^{-t_0 w} \approx e^{t_0 d} \left(\frac{\Lambda_{\text{QCD}}^2}{\mu^2} \right)^{t_0}. \quad (28)$$

Therefore, renormalon ambiguities that arise from the singularities in $T(t, \tau)$ that are located at larger values of t or τ are suppressed by powers of Λ_{QCD}/μ . We can estimate the renormalon ambiguity from the first subleading singularities in $T(t, \tau)$ which are located at $t = 3/2$ or $\tau = 3/2$,

$$\lim_{t \rightarrow 3/2} (3/2 - t) T(t, \tau) = \frac{2(1 - 2\tau)}{\pi} \sin(\pi\tau), \quad (29a)$$

$$\lim_{\tau \rightarrow 3/2} (3/2 - \tau) T(t, \tau) = \frac{2(1 - 2t)}{\pi} \sin(\pi t). \quad (29b)$$

The estimated renormalon ambiguity in $\Gamma_{Q\bar{Q}_1(^1S_0)}$ from the first subleading singularities is

$$\begin{aligned} \delta\Gamma_{Q\bar{Q}_1(^1S_0)} &\sim \left| 2 \times 2\pi i \times \frac{2\pi C_F \alpha_s^2}{m^2} \frac{1}{(\alpha_s \beta_0)^2} \int_0^\infty dt e^{-w(3/2+t)} \frac{2(1 - 2t)}{\pi} \sin(\pi t) \right| \\ &= \frac{2\pi C_F \alpha_s^2}{m^2} \frac{8\pi [1 - 2\alpha_s \beta_0 (2 + d) + (\alpha_s \beta_0)^2 (\pi^2 + d^2 + 4d)]}{[1 - 2\alpha_s \beta_0 d + (\alpha_s \beta_0)^2 (\pi^2 + d^2)]^2} e^{-\frac{3}{2}w}. \end{aligned} \quad (30)$$

This ambiguity is of relative order 10^{-1} for η_c and is of relative order 10^{-3} for η_b . For η_c , the ambiguity is comparable to the nominal size of the order- v^4 correction to the decay rate, and for η_b , the ambiguity is smaller than the nominal size of the order- v^4 correction. Hence, the ambiguity from the subleading renormalon singularities in $T(t, \tau)$ can be neglected at the current level of accuracy.

C. Computation in perturbative NRQCD

The renormalon ambiguities in the perturbation series of $\Gamma_{Q\bar{Q}_1(^1S_0)}$ originate from integrations near zero loop momentum. In the NRQCD factorization formula [Eq. (3)], the contributions from small momentum degrees of freedom are completely contained in the LDMEs. Hence, we expect the loop corrections to the NRQCD LDMEs in the right-hand side of Eq. (3), combined with the SDCs, to reproduce the same renormalon ambiguities in $\Gamma_{Q\bar{Q}_1(^1S_0)}$. In this section, we compute the NRQCD LDMEs in Eq. (3).

Because we set the relative momentum between the Q and the \bar{Q} to be zero, on the right-hand side of Eq. (3), only the matrix element $\langle Q\bar{Q}_1(^1S_0) | \mathcal{O}_1(^1S_0) | Q\bar{Q}_1(^1S_0) \rangle$ appears at order α_s^0 . At order α_s , the matrix element $\langle Q\bar{Q}_1(^1S_0) | \mathcal{O}_8(^3S_1) | Q\bar{Q}_1(^1S_0) \rangle$ appears too. Since we only consider the NRQCD operators of the lowest mass dimensions, the contributions from the right-hand side of Eq. (3) will only reproduce the leading renormalon ambiguity in Eq. (24).

At leading order in α_s , the color-singlet LDME is given by

$$\langle Q\bar{Q}_1(^1S_0) | \mathcal{O}_1(^1S_0) | Q\bar{Q}_1(^1S_0) \rangle = 2N_c. \quad (31)$$

The color-octet matrix element vanishes at order α_s^0 , but it receives contributions at order α_s from the insertion of the $\sigma \cdot \mathbf{B}$ vertices to the quark and antiquark lines. The corresponding Feynman diagrams are shown in Fig. 2. The sum of the diagrams gives

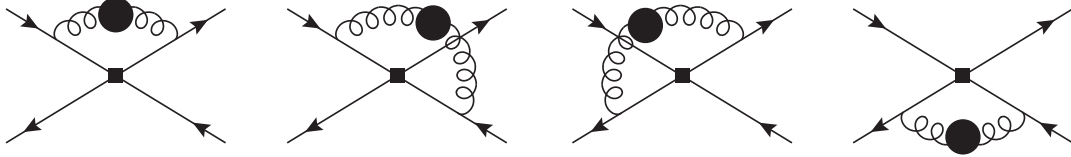


FIG. 2. Feynman diagrams that contribute to $\langle \mathcal{O}_8(^3S_1) \rangle_{Q\bar{Q}_1(^1S_0)}$ at leading order in α_s in perturbative NRQCD. Curly lines with filled circles represent bubble-chain gluons and the filled squares represent the operator $\mathcal{O}_8(^3S_1)$.

$$\langle \mathcal{O}_8(^3S_1) \rangle_{Q\bar{Q}_1(^1S_0)} = I \times \langle \mathcal{O}_1(^1S_0) \rangle_{Q\bar{Q}_1(^1S_0)} + \mathcal{O}(\alpha_s^2), \quad (32)$$

where

$$I = 4g^2 \frac{C_F}{2N_c} \int \frac{d^4k}{(2\pi)^4} iK(x) \left(\frac{1}{-k_0 - \frac{k^2}{2m} + i\epsilon} \right)^2 \frac{k^2}{2m^2}. \quad (33)$$

Here, we use the following shorthand notation $\langle Q\bar{Q}_1(^1S_0) | \mathcal{O}_1(^1S_0) | Q\bar{Q}_1(^1S_0) \rangle = \langle \mathcal{O}_1(^1S_0) \rangle_{Q\bar{Q}_1(^1S_0)}$ and $\langle Q\bar{Q}_1(^1S_0) | \mathcal{O}_8(^3S_1) | Q\bar{Q}_1(^1S_0) \rangle = \langle \mathcal{O}_8(^3S_1) \rangle_{Q\bar{Q}_1(^1S_0)}$. If we rewrite $K(x)$ as

$$iK^{(n)}(x) = -i(\alpha_s\beta_0)^n \left(\frac{d}{dt} \right)^n \frac{(4m^2)^t e^{td}}{(-k^2 - i\epsilon)^{1+t}} \Big|_{t=0}, \quad (34)$$

we can deform the contour for the integration over k_0 so that

$$\begin{aligned} I &= 8g^2 \frac{C_F}{2N_c} \sum_{n=0}^{\infty} (\alpha_s\beta_0)^n \left(\frac{d}{dt} \right)^n \frac{\pi(4m^2)^t e^{td}}{\Gamma(-t)\Gamma(1+t)} \\ &\times \int \frac{d^3\mathbf{k}}{(2\pi)^3} \int_{|\mathbf{k}|}^{\infty} \frac{dk_0}{2\pi} \frac{1}{(k_0^2 - \mathbf{k}^2)^{1+t}} \\ &\times \left(\frac{1}{-k_0 - \frac{k^2}{2m} + i\epsilon} \right)^2 \frac{k^2}{2m^2} \Big|_{t=0}. \end{aligned} \quad (35)$$

We first integrate over k_0 . The result is

$$\begin{aligned} &\int_{|\mathbf{k}|}^{\infty} \frac{dk_0}{2\pi} \frac{1}{(k_0^2 - \mathbf{k}^2)^{1+t}} \left(\frac{1}{-k_0 - \frac{k^2}{2m} + i\epsilon} \right)^2 \\ &= \frac{1}{2\pi|\mathbf{k}|^{3+2t}} J\left(t; \frac{|\mathbf{k}|}{2m}\right), \end{aligned} \quad (36)$$

where

$$\begin{aligned} J(t; z) &= \frac{z}{(1-z^2)^{t+2}} \Gamma(t+2)\Gamma(-t) + \frac{\Gamma(-t)\Gamma(t+\frac{3}{2})}{\Gamma(\frac{1}{2})} \\ &\times F\left(1, t+\frac{3}{2}; \frac{1}{2}; z^2\right). \end{aligned} \quad (37)$$

Here, $F(a, b; c; z)$ is the hypergeometric function. Because we are matching QCD with NRQCD, we expand in $1/m$ and keep only the contribution at leading power in $1/m$ [2],

$$\begin{aligned} I &= 8g^2 \frac{C_F}{2N_c} \sum_{n=0}^{\infty} (\alpha_s\beta_0)^n \left(\frac{d}{dt} \right)^n (4m^2)^{t-1} e^{td} \frac{\Gamma(t+\frac{3}{2})}{\Gamma(1+t)\Gamma(\frac{1}{2})} \\ &\times \int \frac{d^3\mathbf{k}}{(2\pi)^3} \frac{1}{|\mathbf{k}|^{1+2t}} \Big|_{t=0} \\ &= 32\pi\alpha_s \frac{C_F}{2N_c} \frac{1}{\alpha_s\beta_0} \int_0^{\infty} dt e^{-wt} (4m^2)^{t-1} \frac{\Gamma(t+\frac{3}{2})}{\Gamma(1+t)\Gamma(\frac{1}{2})} \\ &\times \int \frac{d^3\mathbf{k}}{(2\pi)^3} \frac{1}{|\mathbf{k}|^{1+2t}}. \end{aligned} \quad (38)$$

In dimensional regularization, the integral over \mathbf{k} is scaleless, and hence vanishes,

$$\begin{aligned} \int \frac{d^3\mathbf{k}}{(2\pi)^3} \frac{1}{|\mathbf{k}|^{1+2t}} &= \int \frac{d^3\mathbf{k}}{(2\pi)^3} \frac{1}{|\mathbf{k}|^{1+2t}} = \frac{1}{2\pi^2} \int_0^1 d|\mathbf{k}| |\mathbf{k}|^{1-2t} \\ &+ \frac{1}{2\pi^2} \int_1^{\infty} d|\mathbf{k}| |\mathbf{k}|^{1-2t} \\ &= \frac{1}{4\pi^2} \left(\frac{1}{1-t} - \frac{1}{1-t} \right), \end{aligned} \quad (39)$$

where in the second equality we split the integral over $|\mathbf{k}|$ so that the first (second) integral corresponds to the region where $|\mathbf{k}|$ is small (large). The first (second) integral is finite only when $t < 1$ ($t > 1$). After integrating over $|\mathbf{k}|$, we use analytical continuation to extend the region of t to the whole complex plane. Since the first term in the parenthesis comes from the region where $|\mathbf{k}|$ is small, and the second term originates from the region where $|\mathbf{k}|$ is large, the first and second terms in the parenthesis correspond to the IR and UV renormalon singularities of the LDME $\langle \mathcal{O}_8(^3S_1) \rangle_{Q\bar{Q}_1(^1S_0)}$, respectively. Then, we can write the right-hand side of Eq. (3) as

$$\begin{aligned} &2\text{Im} \left[\frac{f_1(^1S_0)}{m^2} \right] \langle \mathcal{O}_1(^1S_0) \rangle_{Q\bar{Q}_1(^1S_0)} + 2\text{Im} \left[\frac{f_8(^3S_1)}{m^2} \right] \\ &\times \langle \mathcal{O}_8(^3S_1) \rangle_{Q\bar{Q}_1(^1S_0)} \\ &= 2N_c \times 2\text{Im} \left[\frac{f_1(^1S_0)}{m^2} \right] + 2N_c \times \frac{\pi C_F \alpha_s^2}{N_c m^2} \frac{1}{(\alpha_s\beta_0)^2} \\ &\times \int_0^{\infty} dt \int_0^{\infty} d\tau e^{-w(t+\tau)} T_8^{\text{DR}}(t, \tau), \end{aligned} \quad (40)$$

where

$$T_8^{\text{DR}}(t, \tau) = -\frac{3}{\pi} \sin(\pi\tau) \left[\frac{1}{(1-t)_{\text{IR}}} - \frac{1}{(1-t)_{\text{UV}}} \right] - \frac{3}{\pi} \sin(\pi t) \left[\frac{1}{(1-\tau)_{\text{IR}}} - \frac{1}{(1-\tau)_{\text{UV}}} \right]. \quad (41)$$

The subscripts IR and UV denote the origins of the IR and UV renormalon singularities, respectively. Note that to derive Eq. (40) we rewrote Eq. (12) as

$$2\text{Im} \left[\frac{f_8(^3S_1)}{m^2} \right] = -\frac{2g^2}{4m^2\alpha_s\beta_0} \int_0^\infty d\tau e^{-w\tau} \sin(\pi\tau), \quad (42)$$

and symmetrized in t and τ . By comparing Eq. (40) with Eq. (24), we can see that the infrared renormalon singularities in $T_8^{\text{DR}}(t, \tau)$ [terms proportional to $1/(1-t)_{\text{IR}}$ and $1/(1-\tau)_{\text{IR}}$] reproduce the leading renormalon singularities in $T(t, \tau)$ at $t=1$ or $\tau=1$, and, therefore, Eq. (40) reproduces the leading renormalon ambiguity in Eq. (24). Then, the SDC $2\text{Im}[f_1(^1S_0)/m^2]$, given by

$$2\text{Im} \left[\frac{f_1(^1S_0)}{m^2} \right] = \frac{\pi C_F \alpha_s^2}{N_c m^2} \frac{1}{(\alpha_s \beta_0)^2} \int_0^\infty dt \int_0^\infty d\tau e^{-w(t+\tau)} \times [T(t, \tau) - T_8^{\text{DR}}(t, \tau)], \quad (43)$$

is free of the leading infrared renormalon ambiguity. On the other hand, the UV renormalon singularities in $T_8^{\text{DR}}(t, \tau)$ [terms proportional to $1/(1-t)_{\text{UV}}$ and $1/(1-\tau)_{\text{UV}}$] has no counterpart in perturbative QCD [Eq. (24)]; therefore, the SDC $2\text{Im}[f_1(^1S_0)/m^2]$ has a UV renormalon ambiguity. Since the UV renormalon ambiguity is absent in Eq. (24), the UV renormalon ambiguities in the SDC $2\text{Im}[f_1(^1S_0)/m^2]$ and the LDME $\langle \mathcal{O}_8(^3S_1) \rangle_{Q\bar{Q}, (^1S_0)}$ cancel in the factorization formula Eq. (3). Since the UV renormalon ambiguities are of ultraviolet origin, the nonperturbative LDME $\langle \eta_Q | \mathcal{O}_8(^3S_1) | \eta_Q \rangle$ has the same UV renormalon ambiguities as the perturbative LDME $\langle \mathcal{O}_8(^3S_1) \rangle_{Q\bar{Q}, (^1S_0)}$, with the perturbative $Q\bar{Q}$ states replaced by the nonperturbative meson state. Therefore, the ambiguity is absent in the factorization formula for the inclusive decay rate of η_Q [Eq. (1)].

Even though the UV renormalon ambiguities cancel in the factorization formula, it is still necessary to define the SDC $2\text{Im}[f_1(^1S_0)/m^2]$ and the LDME $\langle \eta_Q | \mathcal{O}_8(^3S_1) | \eta_Q \rangle$ unambiguously in order to compute the inclusive decay rate. An unambiguously defined LDME will lead to an expression for $2\text{Im}[f_1(^1S_0)/m^2]$ that is free of UV renormalon ambiguities; however, different definitions will lead to different expressions for the SDC $2\text{Im}[f_1(^1S_0)/m^2]$ and the LDME $\langle \eta_Q | \mathcal{O}_8(^3S_1) | \eta_Q \rangle$. Especially, the differences

between different definitions of the LDME can be of the size of the UV renormalon ambiguity, which can be estimated from the UV renormalon singularity of $\langle \mathcal{O}_8(^3S_1) \rangle_{Q\bar{Q}, (^1S_0)}$ as

$$\langle \eta_Q | \mathcal{O}_1(^1S_0) | \eta_Q \rangle \times \left| 2 \times 2\pi i \frac{6\alpha_s}{\pi} \frac{C_F}{2N_c} \frac{1}{\alpha_s\beta_0} e^{-w} \right| = \frac{16}{3\beta_0} e^{-w} \langle \eta_Q | \mathcal{O}_1(^1S_0) | \eta_Q \rangle. \quad (44)$$

We note that the renormalon ambiguity scales like $(\Lambda_{\text{QCD}}/\mu)^2$, which is different from velocity-scaling rules of the LDMEs [21]. Hence, there is a possibility that the renormalon ambiguity in the LDMEs can spoil the expansion in powers of v in case the renormalon ambiguity of an LDME exceeds its nominal size.

We can define NRQCD LDMEs so that the LDMEs are free of UV renormalon ambiguities and also respect the velocity-scaling rules by regulating the UV divergences using a cutoff regulator. In perturbative calculations, it is most convenient to apply a hard cutoff Λ on the size of the spatial momentum of the gluon. The cutoff Λ should be large enough so that it encompasses the relevant momentum regions in NRQCD, while $\Lambda < m$ so that the expansion in powers of $1/m$ is valid. Hence, it is customary to choose $\Lambda \sim mv$. While the NRQCD LDMEs in hard-cutoff regularization are free of renormalon ambiguities, they depend on the cutoff Λ .

If we regularize the UV divergences in NRQCD with a hard cutoff Λ for the spatial momentum of the gluon, the integral over \mathbf{k} in Eq. (39) now becomes

$$\int^\Lambda \frac{d^3\mathbf{k}}{(2\pi)^3} \frac{1}{k^{1+2t}} = \frac{4\pi}{(2\pi)^3} \int_0^\Lambda d|\mathbf{k}| |\mathbf{k}|^{1-2t} = \frac{1}{4\pi^2} \frac{\Lambda^{2-2t}}{1-t}, \quad (45)$$

which yields

$$I^{(\Lambda)} = \frac{8\alpha_s}{\pi} \frac{C_F}{2N_c} \frac{1}{\alpha_s\beta_0} \int_0^\infty dt e^{-wt} \frac{\Gamma(t + \frac{3}{2})}{\Gamma(1+t)\Gamma(\frac{1}{2})} \times \left(\frac{\Lambda}{2m} \right)^{2-2t} \frac{1}{1-t}. \quad (46)$$

Here, the superscript (Λ) denotes that a UV cutoff was used. Then, the right-hand side of Eq. (3) reads

$$2\text{Im} \left[\frac{f_1(^1S_0)}{m^2} \right] \langle \mathcal{O}_1(^1S_0) \rangle_{Q\bar{Q}, (^1S_0)} + 2\text{Im} \left[\frac{f_8(^3S_1)}{m^2} \right] \times \langle \mathcal{O}_8(^3S_1) \rangle_{Q\bar{Q}, (^1S_0)} = 2N_c \times 2\text{Im} \left[\frac{f_1(^1S_0)}{m^2} \right] + 2N_c \times \frac{\pi C_F \alpha_s^2}{N_c m^2} \frac{1}{(\alpha_s \beta_0)^2} \times \int_0^\infty dt \int_0^\infty d\tau e^{-w(t+\tau)} T_8^{(\Lambda)}(t, \tau), \quad (47)$$

where

$$T_8^{(\Lambda)}(t, \tau) = \frac{\sin(\pi\tau)}{\pi} \frac{-4\Gamma(t + \frac{3}{2})}{\Gamma(1+t)\Gamma(\frac{1}{2})} \left(\frac{\Lambda}{2m}\right)^{2-2t} \frac{1}{1-t} \\ + \frac{\sin(\pi t)}{\pi} \frac{-4\Gamma(\tau + \frac{3}{2})}{\Gamma(1+\tau)\Gamma(\frac{1}{2})} \left(\frac{\Lambda}{2m}\right)^{2-2\tau} \frac{1}{1-\tau}. \quad (48)$$

As we have discussed in Sec. II A, the SDC $2\text{Im}[g_1(^1S_0)/m^4]$ does not appear in Eq. (47) because the contribution from the LDME $\langle Q\bar{Q}_1(^1S_0)|\mathcal{P}_1(^1S_0)|Q\bar{Q}_1(^1S_0)\rangle$ to the right-hand side of Eq. (3) vanishes at order α_s^2 if the $Q\bar{Q}$ is in the color-singlet 1S_0 state and the relative momentum between the Q and the \bar{Q} is zero. The singularities of $T_8^{(\Lambda)}(t, \tau)$ at $t = 1$ or $\tau = 1$ are given by

$$\lim_{t \rightarrow 1} (1-t)T_8^{(\Lambda)}(t, \tau) = -\frac{3}{\pi} \sin(\pi\tau), \quad (49a)$$

$$\lim_{\tau \rightarrow 1} (1-\tau)T_8^{(\Lambda)}(t, \tau) = -\frac{3}{\pi} \sin(\pi t), \quad (49b)$$

which reproduce the leading renormalon singularities in $T(t, \tau)$ at $t = 1$ or $\tau = 1$. It is clear that, from the expression for $T_8^{(\Lambda)}(t, \tau)$, these are the only singularities at $t > 0$ and $\tau > 0$. Therefore, we define the NRQCD LDME with a UV cutoff Λ to obtain unambiguous expressions for the SDC $2\text{Im}[f_1(^1S_0)/m^2]$.

D. Summary of results

Here we summarize our result for the SDC $2\text{Im}[f_1(^1S_0)/m^2]$. The left-hand side of Eq. (3), computed in perturbative QCD for the $Q\bar{Q}$ in the color-singlet spin-singlet S -wave state, is given in Eq. (24). The right-hand side computed in perturbative NRQCD is given in Eq. (40), when dimensionally regularized, and in Eq. (47), when a hard cutoff is employed. We continue with the latter, which does not require any further subtraction of UV renormalons in perturbative NRQCD. Then, by comparing Eq. (24) with Eq. (47), we obtain

$$2\text{Im}\left[\frac{f_1(^1S_0)}{m^2}\right] = \frac{\pi C_F \alpha_s^2}{N_c m^2} \frac{1}{(\alpha_s \beta_0)^2} \int_0^\infty dt \int_0^\infty d\tau e^{-w(t+\tau)} \\ \times [T(t, \tau) - T_8^{(\Lambda)}(t, \tau)]. \quad (50)$$

Since the functions $T(t, \tau)$ and $T_8^{(\Lambda)}(t, \tau)$ have same singularities at $t = 1$ or $\tau = 1$ [Eqs. (26), (49)], those singularities cancel in $T(t, \tau) - T_8^{(\Lambda)}(t, \tau)$. Therefore, the leading renormalon ambiguities in $\Gamma_{Q\bar{Q}_1(^1S_0)}$ that originate from the singularities at $t = 1$ or $\tau = 1$ are absent in the SDC $2\text{Im}[f_1(^1S_0)/m^2]$.

Together with our results for $2\text{Im}[f_1(^1S_0)/m^2]$ and the perturbative expression for $2\text{Im}[f_{\text{EM}}(^1S_0)/m^2]$ at LO in α_s [2], we obtain the resummed expression for R at leading order in v including resummed QCD corrections in the large n_f limit,

$$R^{\text{Resum}} = R_0[1 + O(v^2)] \times \frac{1}{(\alpha_s \beta_0)^2} \int_0^\infty dt \int_0^\infty d\tau e^{-w(t+\tau)} \\ \times [T(t, \tau) - T_8^{(\Lambda)}(t, \tau)], \quad (51)$$

where

$$R_0 = \frac{C_F \alpha_s^2}{2N_c \alpha^2 e_Q^4}. \quad (52)$$

Here e_Q is the fractional electric charge of the heavy quark Q . As previously discussed, the order- v^2 correction to R vanishes at LO in α_s . We neglect the correction at order $\alpha_s v^2$ that was computed in fixed-order perturbation theory, because it was found to be small numerically [13,17] and is of comparable size to the contribution of order v^3 . The order- v^3 contribution to R can be written as

$$R_8 = -2\text{Im}[4m^2 K(1)] R_0 \frac{N_c}{\alpha_s C_F} \frac{\langle \eta_Q | \mathcal{O}_8(^3S_1) | \eta_Q \rangle}{\langle \eta_Q | \mathcal{O}_1(^1S_0) | \eta_Q \rangle}. \quad (53)$$

Since it is not known how to compute the color-octet LDME $\langle \eta_Q | \mathcal{O}_8(^3S_1) | \eta_Q \rangle$ reliably, we ignore R_8 and instead consider its effects in the uncertainties.

We can combine our results for R^{Resum} with fixed-order calculations of R , so that the corrections at NLO and NNLO in α_s are valid beyond the large n_f limit. By using the expressions for Γ_{η_Q} and $\Gamma_{\eta_Q \rightarrow \gamma\gamma}$ valid to NNLO in α_s , we obtain [11,15,16]

$$R^{\text{Pert}} = R_0 \left\{ 1 + \frac{\alpha_s}{\pi} \left[2\pi \left(\beta_0 - \frac{n_H}{6\pi} \right) \log \frac{\mu^2}{4m^2} + \hat{R}^{(1)} \right] \right. \\ + \left(\frac{\alpha_s}{\pi} \right)^2 \left[3\pi^2 \left(\beta_0 - \frac{n_H}{6\pi} \right)^2 \log^2 \frac{\mu^2}{4m^2} + \hat{R}^{(2)} \right. \\ + \left. \left(2\pi^2 \beta_1 - \frac{19}{12} n_H + 3\pi \left(\beta_0 - \frac{n_H}{6\pi} \right) \hat{R}^{(1)} \right) \log \frac{\mu^2}{4m^2} \right] \\ \left. + O(\alpha_s^3, \alpha_s v^2, v^3) \right\}, \quad (54)$$

where $\hat{R}^{(1)} = \left(\frac{199}{18} - \frac{13\pi^2}{24}\right)C_A - \frac{8}{9}n_f - \frac{2n_H}{3}\log 2$, $\beta_1 = \frac{1}{(4\pi)^2} \left(\frac{34}{3}C_A^2 - \frac{20}{3}C_A T_R n_f - 4C_F T_R n_f\right)$, and n_H is the number of heavy quark flavors. $\hat{R}^{(2)}$ is known as a function of n_f for the case $n_H = 1$ only. $\hat{R}^{(2)} = 117.144$ for $n_f = 3$ and $\hat{R}^{(2)} = 86.421$ for $n_f = 4$. The large n_f limit of $\hat{R}^{(2)}$ is given

in Ref. [11] as $\lim_{n_f \rightarrow \infty} \hat{R}^{(2)}/n_f^2 = 0.37581(3)$. The full n_f dependence of $\hat{R}^{(2)}$ can be obtained from Refs. [11,16] as

$$\hat{R}^{(2)} = 191.3 - \hat{R}_{\text{lbl}}^{(2)} - 25.07n_f + 0.3758n_f^2, \quad (55)$$

where $\hat{R}_{\text{lbl}}^{(2)} = 0.7313 \times C_F \times \sum_f (e_f/e_Q)^2 + 0.6470 \times C_F n_H$ is the ‘‘light by light’’ contribution to the two-photon decay rate that occurs through $Q\bar{Q} \rightarrow g\bar{g} \rightarrow \gamma\gamma$ via a light quark loop. Here, the sum is over n_f light quark flavors, and e_f is the fractional charge of a light quark of flavor f .

When $n_H = 1$, the heavy quark Q contributes to the renormalization scale dependence of α_s , which cancels the explicit renormalization scale dependence of R^{Pert} from the logarithms of μ/m . It is possible to decouple the heavy quark Q from the running of α_s by using the decoupling relations between α_s for n_f and $n_f + 1$ active quark flavors [26], so that the heavy quark Q does not affect the renormalization scale dependence of R^{Pert} for $\mu < m$. By using Eq. (25) of Ref. [26], we decouple the heavy quark, and then we obtain

$$\begin{aligned} R^{\text{Pert}} = R_0 \left\{ 1 + \frac{\alpha_s}{\pi} \left[2\pi\beta_0 \log \frac{\mu^2}{4m^2} + \hat{R}'^{(1)} \right] \right. \\ \left. + \left(\frac{\alpha_s}{\pi} \right)^2 \left[3\pi^2\beta_0^2 \log^2 \frac{\mu^2}{4m^2} + \hat{R}'^{(2)} \right] \right. \\ \left. + (2\pi^2\beta_1 + 3\pi\beta_0\hat{R}^{(1)}) \log \frac{\mu^2}{4m^2} \right\} + O(\alpha_s^3, \alpha_s v^2, v^3), \quad (56) \end{aligned}$$

where $\hat{R}'^{(1)} = (\frac{199}{18} - \frac{13\pi^2}{24})C_A - \frac{8}{9}n_f$ and $\hat{R}'^{(2)} = \hat{R}^{(2)} + \frac{7}{12} + \frac{19}{6} \log 2 - \frac{1}{3} \log^2 2 + \log 2 \hat{R}^{(1)}$. We use this expression for R^{Pert} when $\mu < m$.

The expression for R^{Pert} in Eq. (54) is obtained from the electromagnetic and inclusive decay rates of η_Q that were calculated in the $\overline{\text{MS}}$ renormalization scheme. In order to make Eq. (54) compatible with the expression for R^{Resum} in Eq. (51), it is necessary to convert Eq. (54) to the hard cutoff scheme. It is possible to perform a finite renormalization of the NRQCD LDMEs from the $\overline{\text{MS}}$ scheme to the cutoff scheme. At leading order in v , the finite renormalization only involves the color-singlet LDME, and the finite renormalization cancels trivially in the ratio R . Even if we include contributions from the order- v^2 LDME, which contributes to $\langle \eta_Q | \mathcal{O}_1(^1S_0) | \eta_Q \rangle$ at order α_s , the expression in Eq. (54) remains unchanged if the corrections of order $\alpha_s^2 v^2$ and of order v^4 are ignored.

Because Eq. (54) is computed by using dimensional regularization, all power divergences are absent in Eq. (54). In the fixed-order perturbation theory calculation using the cutoff-regularization scheme, the color-singlet contribution to R receives power-divergent contribution

from the one-loop correction to the color-octet LDME, which is of relative order $\alpha_s \Lambda^2/m^2$. If we set $\Lambda \sim mv$, this contribution is of relative order $\alpha_s v^2$. For $\alpha_s \sim v$, this is the same size as the color-octet contribution to R , whose relative size is of order v^3 ; for $\alpha_s \sim v^2$, the power-divergent contribution is of relative order v^4 . Therefore, such power-divergent contributions in R^{Pert} can be ignored at the current level of accuracy.

In order to combine the perturbative expression [Eq. (54)] with the resummed result [Eq. (51)], we need to subtract from R^{Resum} the contributions that are already included in the perturbative expression R^{Pert} in order to avoid double counting. Since, in the perturbative calculation, the contribution from the color-octet matrix element is not included, we only need to consider the contribution from $T(t, \tau)$. From the series expansion of $T(t, \tau)$ at $t = \tau = 0$ we find

$$\begin{aligned} \delta R^{\text{Resum}} = R_0 \left[1 + 2(1+d)\alpha_s\beta_0 + \left(3d^2 + 6d + 5 \right. \right. \\ \left. \left. - \frac{2\pi^2}{3} + g_2 \right) (\alpha_s\beta_0)^2 + O(\alpha_s^3) \right], \quad (57) \end{aligned}$$

where g_2 is defined by the integral

$$\begin{aligned} g_2 = - \int_0^1 \frac{dx}{x} (1-x) \int_0^1 \frac{dy}{y} (1-y) \theta(\sqrt{x} + \sqrt{y} - 1) \\ + \int_0^1 \frac{dx}{x} \int_0^1 \frac{dy}{y} [f(x, y) - (1-x)(1-y)] \\ \times \theta(1 - \sqrt{x} - \sqrt{y}). \quad (58) \end{aligned}$$

We evaluate this integral numerically to find $g_2 = -3.22467022(9)$. It can be seen that the bubble-chain resummation reproduces the fixed-order perturbation series in the large n_f limit by comparing the coefficients of $(\alpha_s n_f)^n$ for $n = 1$ and 2 in Eqs. (56) and (57). Equation (57) also reproduces the leading logarithmic contributions in Eq. (56) in the form $(\alpha_s \beta_0 \log \frac{\mu^2}{4m^2})^n$ for $n = 1$ and 2 . In Eq. (56), there is an order-by-order cancellation of the renormalization-scale dependence from the two-loop running of α_s with n_f active quark flavors and the explicit logarithms of μ . On the other hand, in Eq. (57), the cancellation only occurs between the one-loop running of α_s and the leading logarithms $(\alpha_s \beta_0 \log \frac{\mu^2}{4m^2})^n$ for $n = 1$ and 2 . Hence, Eq. (57) reproduces the subleading logarithm $\alpha_s^2 \log \frac{\mu^2}{4m^2}$ in Eq. (56) only in the large n_f limit.

Our combined result for the ratio R , where the resummed result and the fixed-order calculation up to NNLO in α_s are combined, is

$$R^{\text{Resum}+\Delta\text{NNLO}} = R^{\text{Resum}} + R^{\text{Pert}} - \delta R^{\text{Resum}}, \quad (59)$$

where R^{Resum} , R^{Pert} , and δR^{Resum} are given in Eqs. (51), (54), and (57), respectively. For $\mu < m$, we use Eq. (56) instead of Eq. (54) to compute R^{Pert} . We also define $R^{\text{Resum}+\Delta\text{NLO}}$, which is the same as $R^{\text{Resum}+\Delta\text{NNLO}}$, except in $R^{\text{Resum}+\Delta\text{NLO}}$, R^{Pert} and δR^{Resum} are computed to NLO in α_s .

Now we discuss the improvement of the perturbative convergence of the combined result $R^{\text{Resum}+\Delta\text{NNLO}}$ compared to the fixed-order calculation R^{Pert} . While R^{Resum} is valid to all orders in α_s in the large n_f limit, $R^{\text{Resum}+\Delta\text{NNLO}}$ receives radiative corrections from $R^{\text{Pert}} - \delta R^{\text{Resum}}$. Then, the perturbative convergence of $R^{\text{Resum}+\Delta\text{NNLO}}$ is closely related to the agreement between R^{Pert} and δR^{Resum} . If we set $\mu = m$, we obtain for the fixed-order perturbative calculation for η_c ,

$$R_{\eta_c}^{\text{Pert}} = R_0 \left[1 + (9.50 - 0.427n_f) \frac{\alpha_s}{\pi} + (32.9 - 6.73n_f - 0.0802n_f^2) \left(\frac{\alpha_s}{\pi} \right)^2 + O(\alpha_s^3) \right]. \quad (60)$$

This expression is valid for an arbitrary number of light quark flavors n_f , except that we only consider three light quark flavors for the contribution to ‘‘light by light’’ contribution to the two-photon decay rate at NNLO in α_s that occurs through $Q\bar{Q} \rightarrow gg \rightarrow \gamma\gamma$ via a light quark loop, which is proportional to the sum of squares of light quark fractional charges [16]. For the decay of η_b , where we consider four light quark flavors in the light by light contribution, we obtain

$$R_{\eta_b}^{\text{Pert}} = R_0 \left[1 + (9.50 - 0.427n_f) \frac{\alpha_s}{\pi} + (24.6 - 6.73n_f - 0.0802n_f^2) \left(\frac{\alpha_s}{\pi} \right)^2 + O(\alpha_s^3) \right]. \quad (61)$$

On the other hand, δR^{Resum} gives, for both η_c and η_b ,

$$\delta R_{\text{NNA}}^{\text{Resum}} = R_0 \left[1 + (7.04 - 0.427n_f) \frac{\alpha_s}{\pi} + (-21.8 + 2.65n_f - 0.0802n_f^2) \left(\frac{\alpha_s}{\pi} \right)^2 + O(\alpha_s^3) \right], \quad (62a)$$

$$\delta R_{\text{BFG}}^{\text{Resum}} = R_0 \left[1 + (9.04 - 0.427n_f) \frac{\alpha_s}{\pi} + (2.30 + 1.37n_f - 0.0802n_f^2) \left(\frac{\alpha_s}{\pi} \right)^2 + O(\alpha_s^3) \right]. \quad (62b)$$

Here, we chose the gauge-fixing parameter in the BFG method to be $\xi = 1$, which corresponds to the Feynman gauge. As expected, δR^{Resum} reproduces R^{Pert} only in the large n_f limit. While it is not at all surprising that δR^{Resum}

does not reproduce R^{Pert} beyond the large n_f limit, the size of the coefficients of order $\alpha_s^2 n_f$ and $\alpha_s^2 n_f^0$ are quite large in R^{Pert} . If the large n_f limit does not provide a good approximation to the fixed-order calculation, the perturbative convergence of $R^{\text{Pert}} - \delta R^{\text{Resum}}$ can be spoiled. To inspect the agreement between R^{Pert} and δR^{Resum} explicitly, we consider the perturbation series of R^{Pert} and δR^{Resum} with $n_f = 3$ and 4 light quark flavors for the case of η_c and η_b , respectively. For the decay of η_c with $n_f = 3$, we obtain

$$R_{\eta_c}^{\text{Pert}} = R_0 \left[1 + 8.22 \frac{\alpha_s}{\pi} + 12.0 \left(\frac{\alpha_s}{\pi} \right)^2 + O(\alpha_s^3) \right], \quad (63a)$$

$$\delta R_{\eta_c, \text{NNA}}^{\text{Resum}} = R_0 \left[1 + 5.76 \frac{\alpha_s}{\pi} - 14.6 \left(\frac{\alpha_s}{\pi} \right)^2 + O(\alpha_s^3) \right], \quad (63b)$$

$$\delta R_{\eta_c, \text{BFG}}^{\text{Resum}} = R_0 \left[1 + 7.76 \frac{\alpha_s}{\pi} + 5.67 \left(\frac{\alpha_s}{\pi} \right)^2 + O(\alpha_s^3) \right]. \quad (63c)$$

For the decay of η_b with $n_f = 4$, we obtain

$$R_{\eta_b}^{\text{Pert}} = R_0 \left[1 + 7.80 \frac{\alpha_s}{\pi} - 3.61 \left(\frac{\alpha_s}{\pi} \right)^2 + O(\alpha_s^3) \right], \quad (64a)$$

$$\delta R_{\eta_b, \text{NNA}}^{\text{Resum}} = R_0 \left[1 + 5.33 \frac{\alpha_s}{\pi} - 12.5 \left(\frac{\alpha_s}{\pi} \right)^2 + O(\alpha_s^3) \right], \quad (64b)$$

$$\delta R_{\eta_b, \text{BFG}}^{\text{Resum}} = R_0 \left[1 + 7.33 \frac{\alpha_s}{\pi} + 6.48 \left(\frac{\alpha_s}{\pi} \right)^2 + O(\alpha_s^3) \right]. \quad (64c)$$

In all cases, agreement between R^{Pert} and δR^{Resum} is poor at NNLO in α_s , even though the difference vanishes in the large n_f limit. Hence, perturbative corrections may not still be in control because of the large radiative corrections in $R^{\text{Resum}+\Delta\text{NNLO}}$ beyond the large n_f limit.

III. NUMERICAL RESULTS

We now discuss our numerical results, based on our expression of R in Eq. (59). We first describe our numerical inputs. We take the heavy-quark mass m to be 1.5 GeV for the charm quark, and 4.6 GeV for the bottom quark. These values are numerically close to the one-loop pole mass. We have a freedom in choosing the values of the heavy-quark mass due to the ambiguity in the pole mass that is of the order of Λ_{QCD} . The quantity R^{Resum} depends on the heavy-quark mass only through $\log \frac{\mu^2}{4m^2}$. Hence, the dependence on the choice of the value of the heavy-quark mass m is

beyond our accuracy. We take the number of light quark flavors to be $n_f = 3$ for η_c and $n_f = 4$ for η_b . In evaluating R^{Resum} , we consider both the NNA and the BFG method. The NRQCD cutoff Λ must be chosen between mv and m , where $v^2 \sim 0.3$ for η_c and $v^2 \sim 0.1$ for η_b . Accordingly, we set the central value for the NRQCD cutoff to be 1 GeV for η_c , and 2 GeV for η_b . We take the central value for μ to be the heavy-quark mass. We compute α_s in the $\overline{\text{MS}}$ renormalization scheme using the `Mathematica` package `RunDec` [26]. We use $\alpha = 1/137.036$. In the BFG method, we set $\xi = 1$, which corresponds to the Feynman gauge. The choice $\xi = 1$ also minimizes the size of the fixed-order corrections $R^{\text{Pert}} - \delta R^{\text{Resum}}$ [see Eqs. (63), (64)]. In evaluating R^{Pert} , we use the expression in Eq. (54) for $\mu \geq m$ and use the expression in Eq. (56) for $\mu < m$.

We list the sources of uncertainties that we consider. We vary Λ by $\pm 25\%$ of its central value. We vary μ between 1 and 2 GeV for η_c , and between 2 and 6 GeV for η_b . Because our expression for R in Eq. (59) only depends on the heavy-quark mass through $\log \frac{\mu^2}{4m^2}$, where μ is the renormalization scale in the $\overline{\text{MS}}$ scheme, the dependence of R on m is very mild. Also, the change in R from varying m is equivalent to the change in R from varying μ . Since we already take into account the uncertainty from the dependence on μ , we ignore the uncertainty from the dependence on m . Finally, we estimate the color-octet LDME by using the perturbative estimate given in Ref. [5],

$$\frac{\langle \eta_Q | \mathcal{O}_8(^3S_1) | \eta_Q \rangle}{\langle \eta_Q | \mathcal{O}_1(^1S_0) | \eta_Q \rangle} \sim \frac{v^3 C_F}{\pi N_c}, \quad (65)$$

where we choose $v^2 = 0.3$ for η_c , and $v^2 = 0.1$ for η_b . The uncertainty from ignoring the color-octet contribution is then estimated by $\pm |R_8|$, where R_8 is given by Eq. (53). Note that the color-octet matrix element $\langle \eta_Q | \mathcal{O}_8(^3S_1) | \eta_Q \rangle$ depends on Λ ; hence, there is a correlation between errors from varying Λ and ignoring the color-octet matrix element. We, however, ignore the correlation and add the uncertainties in quadrature.

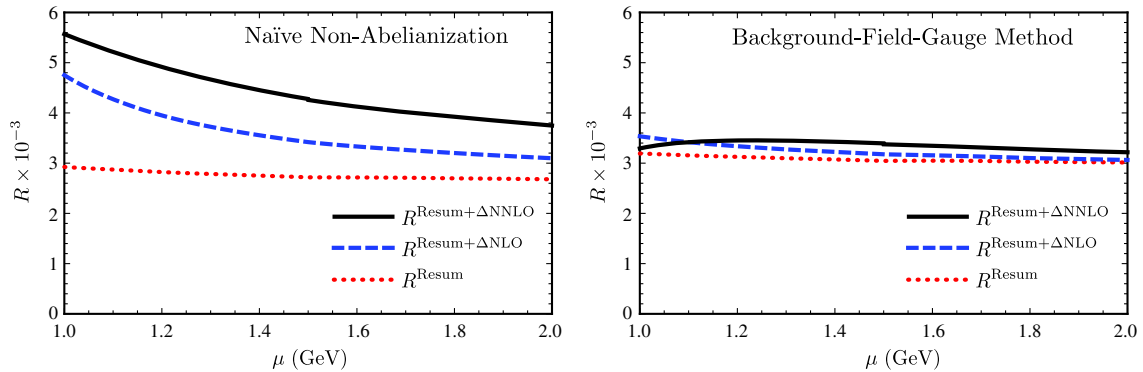


FIG. 3. The renormalization scale dependence of R^{Resum} (dotted line), $R^{\text{Resum}+\Delta\text{NLO}}$ (dashed line) and $R^{\text{Resum}+\Delta\text{NNLO}}$ (black line) for η_c and $\Lambda = 1$ GeV, for the NNA (left) and the BFG method (right).

A. Decay of η_c

We first present our numerical results for the ratio R for η_c . In Fig. 3, we show the dependence on the renormalization scale μ of R^{Resum} , $R^{\text{Resum}+\Delta\text{NLO}}$ and $R^{\text{Resum}+\Delta\text{NNLO}}$ at $\Lambda = 1$ GeV. For both the NNA and BFG methods, R^{Resum} has some dependence on μ because the renormalization scale dependence in R^{Resum} only cancels at the one-loop level. For the case of NNA, $R^{\text{Resum}+\Delta\text{NLO}}$ develops a stronger dependence on μ from the fixed-order corrections of relative order α_s in $R^{\text{Pert}} - \delta R^{\text{Resum}}$. In $R^{\text{Resum}+\Delta\text{NNLO}}$, the renormalization scale dependence is slightly worse than $R^{\text{Resum}+\Delta\text{NLO}}$, because of the subleading logarithm of the form $\alpha_s^2 \log \frac{\mu^2}{4m^2}$ in $R^{\text{Pert}} - \delta R^{\text{Resum}}$. For $\mu > m$, there are also uncanceled leading logarithms in $R^{\text{Pert}} - \delta R^{\text{Resum}}$ that are proportional to n_H . For the case of the BFG method, R^{Resum} , $R^{\text{Resum}+\Delta\text{NLO}}$ and $R^{\text{Resum}+\Delta\text{NNLO}}$ all depend on μ very mildly. This is because in the BFG method in the Feynman gauge, there is almost exact cancellation in the fixed-order corrections $R^{\text{Pert}} - \delta R^{\text{Resum}}$, which contain most of the dependence on μ .

In Fig. 4 we show the dependence on the NRQCD cutoff Λ of R^{Resum} , $R^{\text{Resum}+\Delta\text{NLO}}$ and $R^{\text{Resum}+\Delta\text{NNLO}}$ at $\mu = m$. In all cases, the dependence on Λ is mild, and the numerical values of R rise slowly with increasing Λ . As we will see later, the uncertainty estimated from varying Λ is smaller than the estimated uncertainty from neglecting the color-octet contribution.

For $\mu = m$, the fixed-order corrections in $R^{\text{Pert}} - \delta R^{\text{Resum}}$ are positive for both the contributions of relative order α_s and order α_s^2 . In NNA, $R^{\text{Resum}+\Delta\text{NLO}}$ is larger than R^{Resum} by about 16% of the central value of $R^{\text{Resum}+\Delta\text{NNLO}}$, and $R^{\text{Resum}+\Delta\text{NNLO}}$ is larger than $R^{\text{Resum}+\Delta\text{NLO}}$ by about 20% of the central value of $R^{\text{Resum}+\Delta\text{NNLO}}$. In the BFG method, $R^{\text{Resum}+\Delta\text{NLO}}$ is larger than R^{Resum} by about 4% of the central value of $R^{\text{Resum}+\Delta\text{NNLO}}$, and $R^{\text{Resum}+\Delta\text{NNLO}}$ is larger than $R^{\text{Resum}+\Delta\text{NLO}}$ by about 6% of the central value of $R^{\text{Resum}+\Delta\text{NNLO}}$. While the effects of the fixed-order corrections appear less dramatic than the effects of the radiative

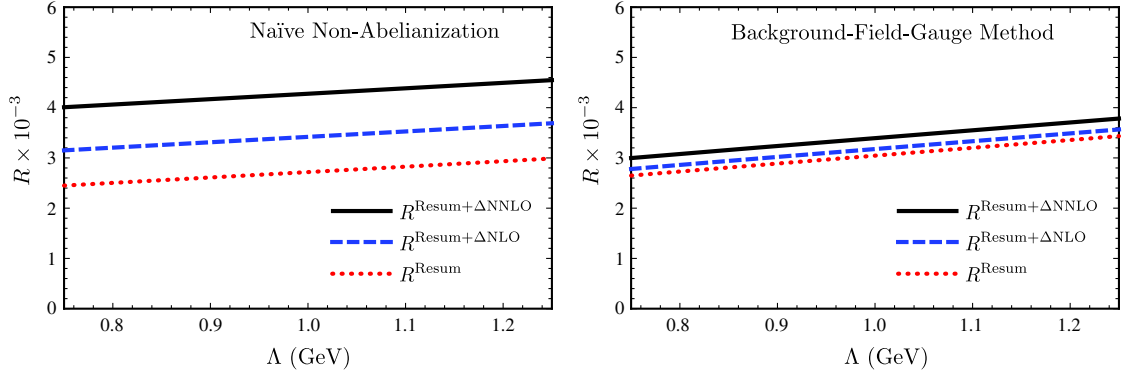


FIG. 4. The NRQCD cutoff dependence of R^{Resum} (dotted line), $R^{\text{Resum}+\Delta\text{NLO}}$ (dashed line) and $R^{\text{Resum}+\Delta\text{NNLO}}$ (black line) for η_c and $\mu = m$ for the NNA (left) and the BFG method (right).

corrections in the fixed-order calculation in Ref. [11], the fact that the corrections are larger at NNLO than at NLO in α_s , implies that the perturbative corrections may still not be under control. As discussed in the previous section, this is related to the large perturbative corrections in the fixed-order corrections that go beyond the large n_f limit; because the treatment of the renormalon ambiguities in this work is only valid in the large n_f limit, we have little or no control over the convergence of the perturbation series beyond the large n_f limit.

We estimate the uncertainties by varying μ between 1 and 2 GeV, and by varying Λ between 0.75 and 1.25 GeV. We also include the uncertainty for ignoring the color-octet contribution. For NNA, we obtain

$$\begin{aligned} R_{\eta_c}^{\text{Resum}+\Delta\text{NNLO}}(\text{NNA}) &= (4.28_{-0.53}^{+1.29} \pm 0.27 \pm 0.41) \times 10^3 \\ &= (4.28_{-0.72}^{+1.38}) \times 10^3, \end{aligned} \quad (66)$$

where the first uncertainty is from μ , the second from Λ , and the third uncertainty is from the neglected color-octet contribution. For BFG, we obtain

$$\begin{aligned} R_{\eta_c}^{\text{Resum}+\Delta\text{NNLO}}(\text{BFG}) &= (3.39_{-0.18-0.40}^{+0.06+0.39} \pm 0.47) \times 10^3 \\ &= (3.39_{-0.64}^{+0.61}) \times 10^3, \end{aligned} \quad (67)$$

where the uncertainties are as in NNA. Our numerical results for the NNA and the BFG methods are compatible within uncertainties. We note that $R^{\text{Resum}+\Delta\text{NNLO}}$ in the NNA method has a large uncertainty from its strong renormalization-scale dependence for small μ .

In estimating the uncertainties in our numerical results we have neglected the possibility that the convergence of the fixed-order corrections in $R^{\text{Pert}} - \delta R^{\text{Resum}}$ may not be in control. We roughly estimate the uncertainty from this nonconvergence by comparing our numerical results for R with the series expansion of $\text{Br}(\eta_c \rightarrow \gamma\gamma) = 1/R_{\eta_c}^{\text{Resum}+\Delta\text{NNLO}}$ in powers of α_s through NNLO accuracy. For NNA, we obtain $\text{Br}_{\text{NNA}}(\eta_c \rightarrow \gamma\gamma) = (5.51 \times 10^3)^{-1}$,

and for BFG, we obtain $\text{Br}_{\text{BFG}}(\eta_c \rightarrow \gamma\gamma) = (3.44 \times 10^3)^{-1}$. These values are in agreement with our numerical results in Eqs. (66) and (67) within uncertainties. Therefore, at the current level of accuracy, the uncertainty from the possible nonconvergence of the fixed-order corrections in $R^{\text{Pert}} - \delta R^{\text{Resum}}$ may not exceed our estimated uncertainties.

We can compare our numerical results with measurements. PDG reports two values for the η_c branching ratio to two photons [6]. The first PDG value $\text{Br}(\eta_c \rightarrow \gamma\gamma) = (1.59 \pm 0.13) \times 10^{-4}$ is from a constrained fit of partial widths. If we take the inverse, we obtain $R_{\text{fit}}^{\text{exp}} = (6.29_{-0.48}^{+0.56}) \times 10^3$. The second PDG value is from an average of measurements, which gives $\text{Br}(\eta_c \rightarrow \gamma\gamma) = (1.9_{-0.6}^{+0.7}) \times 10^{-4}$. Taking the inverse gives $R_{\text{average}}^{\text{exp}} = (5.3_{-1.4}^{+2.4}) \times 10^3$. The two PDG values are compatible with each other due to the large uncertainties in $R_{\text{average}}^{\text{exp}}$. The uncertainty in $R_{\text{fit}}^{\text{exp}}$ is smaller than the uncertainty in $R_{\text{average}}^{\text{exp}}$ or the uncertainties in our numerical results for R . Note that $R_{\text{average}}^{\text{exp}}$ is compatible with our results for R in Eqs. (66) and (67). There is, however, a tension between $R_{\text{fit}}^{\text{exp}}$ and our numerical results. We also note that our calculation of R also applies for the $\eta_c(2S)$ state as well. The PDG value for the $\eta_c(2S)$ branching ratio to two photons is $\text{Br}(\eta_c(2S) \rightarrow \gamma\gamma) = (1.9 \pm 1.3) \times 10^{-4}$, which is compatible with the PDG values for the $\text{Br}(\eta_c \rightarrow \gamma\gamma)$ and our results for R in Eqs. (66) and (67).

B. Decay of η_b

We now present our results for η_b . In Fig. 5, we show the dependence on the renormalization scale μ of R^{Resum} , $R^{\text{Resum}+\Delta\text{NLO}}$ and $R^{\text{Resum}+\Delta\text{NNLO}}$ at $\Lambda = 2$ GeV. Just like for the case of η_c , R^{Resum} has some dependence on μ because the renormalization scale dependence in R^{Resum} only cancels at the one-loop level. For the case of NNA, $R^{\text{Resum}+\Delta\text{NLO}}$ develops a stronger dependence on μ from the fixed-order corrections of relative order α_s in $R^{\text{Pert}} - \delta R^{\text{Resum}}$. This dependence is partially canceled by the corrections of relative order α_s^2 , which contain logarithms

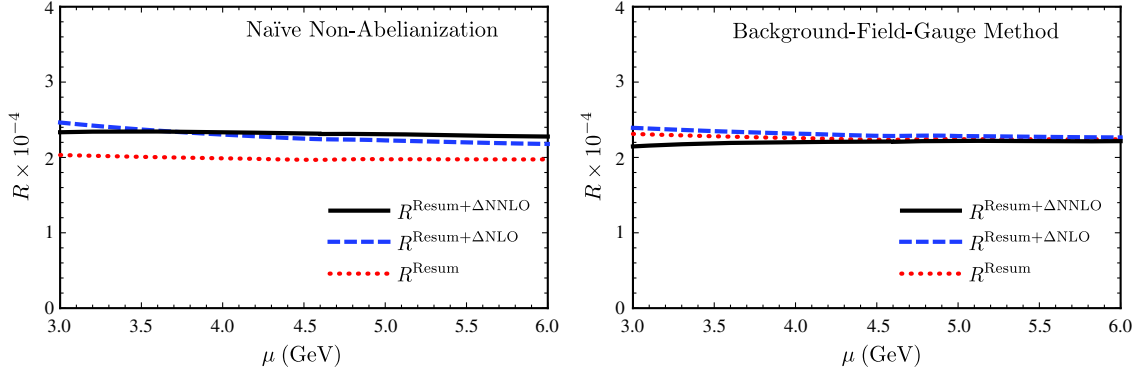


FIG. 5. The renormalization scale dependence of R^{Resum} (dotted line), $R^{\text{Resum}+\Delta\text{NLO}}$ (dashed line) and $R^{\text{Resum}+\Delta\text{NNLO}}$ (black line) for η_b and $\Lambda = 2$ GeV for the NNA (left) and the BFG method (right).

of μ , and $R^{\text{Resum}+\Delta\text{NNLO}}$ depends on μ mildly. For the case of the BFG method, R^{Resum} , $R^{\text{Resum}+\Delta\text{NLO}}$ and $R^{\text{Resum}+\Delta\text{NNLO}}$ all depend on μ mildly. This is again because the choice $\xi = 1$ minimizes the size of the fixed-order corrections $R^{\text{Pert}} - \delta R^{\text{Resum}}$, which contain most of the dependence on μ .

In Fig. 6 we show the dependence on the NRQCD cutoff Λ of R^{Resum} , $R^{\text{Resum}+\Delta\text{NLO}}$ and $R^{\text{Resum}+\Delta\text{NNLO}}$ at $\mu = m$, and $1.5 \text{ GeV} \leq \Lambda \leq 2.5 \text{ GeV}$. In all cases, the dependence on Λ is mild, and the numerical values of R rise very slowly with increasing Λ . Just like for the case of η_c , the uncertainty estimated from varying Λ is smaller than the estimated uncertainty from neglecting the color-octet contribution.

For NNA at $\mu = m$ and $\Lambda = 2$ GeV, the fixed-order corrections in $R^{\text{Pert}} - \delta R^{\text{Resum}}$ are positive for both the contributions of relative order- α_s and order- α_s^2 . In NNA, $R^{\text{Resum}+\Delta\text{NLO}}$ is larger than R^{Resum} by about 11% of the central value of $R^{\text{Resum}+\Delta\text{NNLO}}$, and $R^{\text{Resum}+\Delta\text{NNLO}}$ is larger than $R^{\text{Resum}+\Delta\text{NLO}}$ by about 3% of the central value of $R^{\text{Resum}+\Delta\text{NNLO}}$. In the BFG method, at $\mu = m$ and $\Lambda = 2$ GeV, $R^{\text{Resum}+\Delta\text{NLO}}$ is larger than R^{Resum} by about 2% of the central value of $R^{\text{Resum}+\Delta\text{NNLO}}$, and $R^{\text{Resum}+\Delta\text{NNLO}}$ is smaller than $R^{\text{Resum}+\Delta\text{NLO}}$ by about 3%

of the central value of $R^{\text{Resum}+\Delta\text{NNLO}}$. The effects of the fixed-order corrections are much less dramatic than the corrections to the η_c decay rate, thanks to the smaller size of α_s and larger n_f .

We estimate the uncertainties by varying μ between 3 and 6 GeV, and by varying Λ between 1.5 and 2.5 GeV. We also include the uncertainty for ignoring the color-octet contribution. For NNA, we obtain

$$\begin{aligned} R_{\eta_b}^{\text{Resum}+\Delta\text{NNLO}}(\text{NNA}) &= (2.32_{-0.05}^{+0.02} \pm 0.04 \pm 0.06) \times 10^4 \\ &= (2.32_{-0.09}^{+0.08}) \times 10^4, \end{aligned} \quad (68)$$

where the first uncertainty is from μ , the second from Λ , and the third uncertainty is from the neglected color-octet contribution. For BFG, we obtain

$$\begin{aligned} R_{\eta_b}^{\text{Resum}+\Delta\text{NNLO}}(\text{BFG}) &= (2.41_{-0.05-0.05}^{+0.00+0.06} \pm 0.07) \times 10^4 \\ &= (2.41_{-0.10}^{+0.09}) \times 10^4, \end{aligned} \quad (69)$$

where the uncertainties are as in NNA. Our numerical results for the NNA and the BFG methods are compatible within uncertainties.

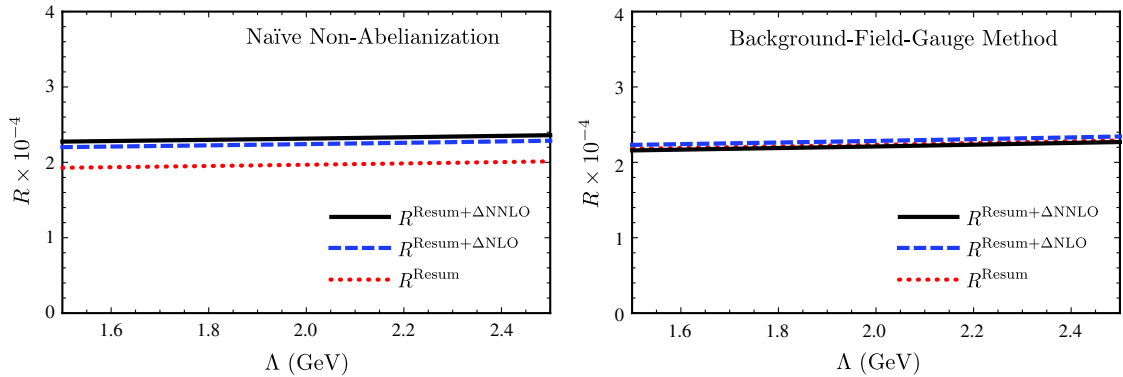


FIG. 6. The NRQCD cutoff dependence of R^{Resum} (dotted line), $R^{\text{Resum}+\Delta\text{NLO}}$ (dashed line) and $R^{\text{Resum}+\Delta\text{NNLO}}$ (black line) for η_b and $\mu = 2$ GeV for the NNA (left) and the BFG method (right).

Even though the fixed-order corrections in $R^{\text{Pert}} - \delta R^{\text{Resum}}$ are not as large as the corrections to the η_c decay rate, our results may still suffer from nonconvergence. We again roughly estimate the uncertainty from this possible nonconvergence by comparing our numerical results for R with the series expansion of $\text{Br}(\eta_b \rightarrow \gamma\gamma) = 1/R_{\eta_b}^{\text{Resum}+\Delta\text{NNLO}}$ in powers of α_s through NNLO accuracy. For NNA, we obtain $\text{Br}_{\text{NNA}}(\eta_b \rightarrow \gamma\gamma) = (2.34 \times 10^4)^{-1}$, and for BFG, we obtain $\text{Br}_{\text{BFG}}(\eta_b \rightarrow \gamma\gamma) = (2.41 \times 10^4)^{-1}$. These values are in good agreement with our numerical results in Eqs. (68) and (69). This may imply that the uncertainty from the possible nonconvergence of the fixed-order corrections in $R^{\text{Pert}} - \delta R^{\text{Resum}}$ is not significant for the case of η_b .

It is not yet possible to compare our results in Eqs. (68) and (69) with measurements because the partial width $\Gamma_{\eta_b \rightarrow \gamma\gamma}$ has not been observed yet. In Ref. [27], the authors made use of the heavy-quark spin symmetry to extract η_b LDMEs from the Υ LDMEs and made the prediction $\Gamma_{\eta_b \rightarrow \gamma\gamma} = 0.512_{-0.094}^{+0.096}$ keV. If we multiply this result to our results for R , we obtain $\Gamma_{\eta_b} = 11.9_{-2.2}^{+2.3}$ MeV for NNA, and $\Gamma_{\eta_b} = 12.4_{-2.3}^{+2.4}$ MeV for the BFG method. Reference [28] makes use of the ratio of the leptonic decay rate of the Υ to the decay rate of η_b into two photons in the potential NRQCD effective field theory to predict $\Gamma_{\eta_b \rightarrow \gamma\gamma}$ from the measured value for $\Gamma_{\Upsilon \rightarrow e^+e^-}$. The prediction in Ref. [28] is given by $\Gamma_{\eta_b \rightarrow \gamma\gamma} = 0.54 \pm 0.15$ keV, which is compatible with the prediction in Ref. [27]. If we use this prediction, we obtain $\Gamma_{\eta_b} = 12.5 \pm 3.5$ MeV for NNA and $\Gamma_{\eta_b} = 13.0 \pm 3.7$ MeV for the BFG method. These predictions for the η_b decay rate are compatible with the PDG value for the η_b decay width, which is given by $\Gamma_{\eta_b} = 10_{-4}^{+5}$ MeV.

C. Comparison with previous results

We now compare our numerical results with previous results for R . In Ref. [5], the authors also considered resummation of bubble-chain contributions to R for the decay of η_c . The results of Ref. [5] are equivalent to $R^{\text{Resum}+\Delta\text{NNLO}}$, except that in Ref. [5], the SDC was computed by imposing a hard IR cutoff which affects both the virtuality and the spacial momentum of the gluon in the perturbative QCD calculation [Eq. (18)]. The authors of Ref. [5] identified the contribution from the momentum region that was neglected in the perturbative QCD calculation as the contribution from perturbative NRQCD which is regulated by a hard UV cutoff on the gluon momentum. The hard cutoff that was used in Ref. [5] is given by $k^2 \leq 4m^2\delta$ and $\mathbf{k}^2 \leq m^2(2\sqrt{\delta} - \delta)^2$, where k is a gluon momentum, and $\delta = 0.1$. If we take $m = 1.5$ GeV, we obtain $k^2 \leq 0.9$ GeV² and $|\mathbf{k}| \leq 0.8$ GeV. Numerically, the hard cutoff imposed on $|\mathbf{k}|$ is similar to the hard UV cutoff Λ that we have employed in this paper, although in this work, there is no cutoff on the virtuality of the gluon. The main advantage

of this work compared to Ref. [5] is that in this work, the appearance and the cancellation of renormalon ambiguities are explicitly shown by employing dimensional regularization to regulate infrared divergences. In the numerical results, we have retained the dependence on the hard cutoff Λ , whereas the authors of Ref. [5] only considered a fixed value of the cutoff. We also include the fixed-order corrections at NNLO accuracy in α_s . The authors of Ref. [5] obtained $R_{\eta_c} = (3.01 \pm 0.30 \pm 0.34) \times 10^3$ for NNA, and $R_{\eta_c} = (3.26 \pm 0.31 \pm 0.47) \times 10^3$ for the BFG method in the Feynman gauge. The result for the BFG method is compatible with our result in Eq. (67), while the result for NNA in Ref. [5] is smaller than our result in Eq. (66) by about 30%. This difference can be understood from the large positive correction at NNLO in α_s from $R^{\text{Pert}} - \delta R^{\text{Resum}}$ that we have included in this paper.

The authors of Ref. [11] presented their numerical results for $\text{Br}(\eta_c \rightarrow \gamma\gamma)$, which is equal to R^{-1} , based on their fixed-order calculation of the inclusive decay rate of η_c and the decay rate of η_c into two photons in Ref. [16] to NNLO accuracy in α_s . The result in Ref. [11] is based on the perturbation expansion of $\text{Br}(\eta_c \rightarrow \gamma\gamma) = R^{-1}$ to NNLO in α_s^2 . By varying the renormalization scale μ from 1 GeV to 3 times the charm quark mass, the authors of Ref. [11] obtained $\text{Br}(\eta_c \rightarrow \gamma\gamma) = (3.1-3.3) \times 10^{-4}$, which gives $R_{\eta_c} = (3.0-3.2) \times 10^3$. This result is compatible with our result in Eq. (67) in the BFG method, but is smaller than our result in Eq. (66) in NNA. Also, the uncertainty in the result in Ref. [11] is smaller than the uncertainties in our results, due to the cancellation of the renormalization-scale dependence at the two-loop level in the fixed-order calculation. Moreover, the uncertainty from the color-octet contribution at relative order v^3 has been neglected in Ref. [11]. One can obtain a different numerical result if one considers the perturbation series of $R_{\eta_c} = [\text{Br}(\eta_c \rightarrow \gamma\gamma)]^{-1}$, which is given by Eq. (54). If we use Eq. (54) we obtain $R_{\eta_c} = 4.9 \times 10^3$ at $\mu = m$. This disagrees with the numerical results in Ref. [11], and the discrepancy is much larger than the uncertainties estimated in Ref. [11] by varying the renormalization scale μ . The difference between the numerical results based on the perturbation series of R_{η_c} and the one based on the perturbation series of $\text{Br}(\eta_c \rightarrow \gamma\gamma)$ shows that the nonconvergence of the perturbation series generates a sizable ambiguity. This is consistent with our estimate of the leading renormalon uncertainty in Eq. (27). Our results in Eqs. (66) and (67) also suffer from nonconvergence of the fixed order corrections in $R^{\text{Pert}} - \delta R^{\text{Resum}}$, because we have no control over the convergence of the perturbation series beyond the large n_f limit. We have roughly estimated the uncertainty from this nonconvergence by comparing our numerical results with the series expansion of $\text{Br}(\eta_c \rightarrow \gamma\gamma) = 1/R_{\eta_c}^{\text{Resum}+\Delta\text{NNLO}}$ in powers of α_s through NNLO accuracy. We have found that our rough estimate of the uncertainty from the nonconvergence does not exceed the uncertainties in our numerical results.

In Ref. [11], the authors also presented their numerical results based on the perturbative expression of $\text{Br}(\eta_b \rightarrow \gamma\gamma)$ to NNLO accuracy. They obtained $\text{Br}(\eta_b \rightarrow \gamma\gamma) = (4.8 \pm 0.7) \times 10^{-5}$. If we take the inverse we obtain $R_{\eta_b} = (2.1_{-0.3}^{+0.4}) \times 10^4$, which is compatible with our numerical results in Eqs. (68) and (69) within uncertainties. The uncertainties in Eqs. (68) and (69) are much smaller than the result in Ref. [11] because the bubble-chain resummation reduces the dependence on the renormalization scale μ compared to the fixed-order calculation. If we use the perturbative expression of R in Eq. (54), which is valid to NNLO accuracy in α_s , we obtain $R_{\eta_b} = 2.39 \times 10^4$ at $\mu = m$, which agrees with the numerical result in Ref. [11] within uncertainties. The relative discrepancy between the numerical result from the perturbative expression of the branching ratio into two photons and the numerical result from the perturbative expression of R is smaller in the case of η_b compared to the case of η_c . This can be understood from our estimate of the leading renormalon ambiguity [Eq. (27)]: since the decay of η_b occurs at a higher energy scale than the decay of η_c , the renormalon ambiguity is suppressed compared to the case of η_c . Nevertheless, the ambiguity is still sizable compared to the estimated uncertainties in our numerical results in Eqs. (68) and (69). Therefore, even for the case of η_b , resumming large perturbative corrections is crucial in obtaining a reliable theoretical prediction.

In Ref. [29], the authors applied the principle of maximal conformality (PMC), which is a method for choosing the renormalization scale μ for a given perturbation series, to the perturbative expression for R to NLO accuracy. The authors of Ref. [29] claim that, by applying the PMC, the β function appearing in the perturbation series, which are associated with the running of α_s , is absorbed into the running coupling, and the convergence of the perturbation series is improved. When they include the relative order- α_s and order- $\alpha_s v^2$ corrections to R , they obtain, after applying the PMC, $R = (6.09_{-0.19-0.52}^{+0.21+0.58}) \times 10^3$. This result is very different from our results in Eqs. (66) and (67), which include explicitly the leading-logarithmic corrections of the form $(\alpha_s \beta_0 \log \frac{\mu^2}{4m^2})^n$ to all orders in α_s . It is worth noting that, unlike the expressions for R at LO and NLO accuracies, the perturbative expression for R at NNLO accuracy no longer suffers from the severe dependence on the renormalization scale [11]. Even if we consider a wide range of the renormalization scale, as the authors of Ref. [11] have done, it is not possible to obtain a value of R that is close to the result of Ref. [29] if one uses the expression for R at NNLO accuracy. Shortcomings of the PMC approach have been discussed in Ref. [30].

IV. SUMMARY AND DISCUSSION

In this paper we have presented an analysis of the ratio R of the inclusive decay rate of the η_Q meson to the partial

decay rate into two photons, where $Q = c$ or b . In the calculation of the short-distance coefficients, we resum large perturbative corrections in the form $(\alpha_s \beta_0)^n$ to all orders in α_s by including contributions from bubble chain insertions in the gluon propagator. This bubble-chain resummation reproduces fixed-order perturbative calculations in the large n_f limit. This resummation has been done in Ref. [5] by imposing an infrared cutoff in the perturbative calculations. In this work, we regulate the infrared divergences using dimensional regularization, so that the appearance of the renormalon ambiguity in the perturbative QCD calculation and the cancellation of the ambiguity in the factorization formula can be seen explicitly. We use naïve non-Abelianization and the background-field gauge method to carry out the resummation, which are unambiguous procedures for resumming bubble chains.

We confirmed that, by using the factorization formula valid to relative order v^3 , the leading renormalon ambiguity of infrared origin that arises from the perturbative QCD calculation is reproduced in the perturbative NRQCD calculation, and therefore, the short-distance coefficients are free of infrared renormalon ambiguities. We also showed that, if we use dimensional regularization to regulate the ultraviolet divergences in NRQCD, the color-octet LDME suffers from renormalon ambiguities of ultraviolet origin, but the ambiguity cancels in the factorization formula. Since it is not known how to compute the color-octet LDME reliably, and it is known that the color-octet LDME is suppressed by v^3 compared to the leading-order color-singlet LDME, the color-octet contribution is often neglected in the factorization formula. However, in a resummed calculation, the neglect of the color-octet contribution results in a sizable ambiguity in the factorization formula. We argued that, for phenomenological applications, we obtain a more useful factorization formula if we use hard-cutoff regularization to regulate the ultraviolet divergences in NRQCD where such ambiguity no longer appears.

Our result for the resummed calculation of R is shown in Eq. (51). We combine our result with the calculation in fixed-order perturbation theory to next-to-next-to-leading order accuracy in α_s [Eq. (54)] [9–11,15,16]. The expression for the combined result is shown in Eq. (59). We use the expression in Eq. (59) in our numerical analysis.

In our numerical analysis, we estimated uncertainties by varying the renormalization scale and the NRQCD ultraviolet cutoff. We also included the effect of the color-octet contribution by estimating the size of the uncalculated color-octet LDME. Our numerical results for the ratio R for the decay of η_c are given in Eqs. (66) and (67), which are computed in the naïve non-Abelianization and the background-field gauge method in the Feynman gauge, respectively. The results in Eqs. (66) and (67) agree within uncertainties. Our numerical results for η_c are compatible with the PDG value for $\text{Br}(\eta_c \rightarrow \gamma\gamma)$ that was obtained

by taking averages of measurements. However, our results disagree with the PDG value for $\text{Br}(\eta_c \rightarrow \gamma\gamma)$ that was obtained from constrained fits. For the decay of η_b , our numerical results for the ratio R are given in Eqs. (68) and (69), which are computed in the naïve non-Abelianization and the background-field gauge method in the Feynman gauge, respectively. Again, the numerical results in Eqs. (68) and (69) agree within uncertainties. Since the decay of η_b into two photons is yet to be measured, we cannot compare our results for R directly with measurements for the case of η_b . By using predictions of $\Gamma_{\eta_b \rightarrow \gamma\gamma}$ in Refs. [27,28], we have obtained predictions of Γ_{η_b} that is compatible with the current measurement of the η_b decay rate.

We have compared our numerical results with previous calculations of R in Ref. [5], where the authors also considered bubble-chain resummation, and the results based on fixed-order perturbation theory in Ref. [11]. In Ref. [5], the authors made predictions of R for the decay of η_c by combining the resummed result, which was computed by using a fixed infrared cutoff, with the fixed-order calculation valid to next-to-leading order in α_s . Our numerical results agree with the results in Ref. [5] for the background-field gauge method [Eq. (67)], but there is tension in the result in naïve non-Abelianization [Eq. (66)]. This discrepancy is mostly from the inclusion of the fixed-order corrections $R^{\text{Pert}} - \delta R^{\text{Resum}}$ at next-to-next-to-leading order in α_s [Eq. (59)]. While the authors of Ref. [5] included the effect of the color-octet contribution in the uncertainties, the uncertainty from the dependence on the infrared cutoff was neglected. The numerical results for R for η_c in Ref. [11] is also compatible with our results in the background-field gauge method [Eq. (67)], but disagrees with our results in naïve non-Abelianization [Eq. (66)]. The uncertainties in the result of Ref. [11] is smaller than the uncertainties in our results because in the fixed-order calculation, the dependence on the renormalization scale cancels at two-loop accuracy, and the uncertainty from the uncalculated color-octet contribution is neglected. Also, the fixed-order calculation in Ref. [11] suffers from a sizable uncertainty from the nonconverging perturbation series, which, for the case of η_c , can be of relative order one. The authors of Ref. [11] also made a prediction of R for the decay of η_b , which agrees with our results in Eqs. (68) and (69) within uncertainties. The uncertainties in our results are smaller than the uncertainty in the prediction from fixed-order perturbation theory in Ref. [11]. Although in the case of η_b , the estimated renormalon ambiguity in the perturbation series for R is smaller than the case of η_c , our estimate of the ambiguity is larger than the uncertainties in our numerical results in Eqs. (68) and (69). Therefore, we conclude that resummation is necessary in order to obtain an accurate prediction of R for the decay of η_b .

In Ref. [29], the authors applied the principle of maximal conformality to the perturbative expression of R for the

decay of η_c valid to next-to-leading order in α_s . The authors of Ref. [29] claimed that a resummed perturbative expression can be obtained, where the β function that is associated with the running of α_s are absorbed into the coupling, by using the principle of maximal conformality. However, we find that our resummed result disagrees with the result in Ref. [29]. The result in Ref. [29] also disagrees with the result from fixed-order perturbation theory valid to next-to-next-to-leading order in α_s in Ref. [11].

It is noticeable that the uncertainty estimated from the neglected color-octet contribution is quite significant for both η_c and η_b . This suggests that in order to have a more precise prediction of R , it is necessary to include color-octet contributions in R . Including the color-octet contribution may also reduce the uncertainty from the NRQCD cutoff dependence, because the dependence on the NRQCD cutoff cancels in the factorization formula between the color-singlet and color-octet contributions. Since currently it is not known how to calculate the color-octet matrix element reliably, it would be important to develop new ideas to investigate the nature of the color-octet matrix element in NRQCD and other effective field theories such as potential NRQCD, which may help constrain the color-octet contribution.

In our numerical results we included corrections from fixed-order calculations to next-to-next-to-leading order in α_s . While the bubble-chain resummation reproduces the fixed-order corrections in the large n_f limit, the fixed-order corrections are still found to be significant beyond the large n_f limit; even after the bubble-chain resummation, the numerical results for R for the decay of η_c suggest non-convergence of perturbative corrections to persist beyond the large n_f limit. Therefore, in order to gain control over the perturbation series of R for the decay of η_c , it may be necessary to consider renormalon ambiguities beyond the large n_f limit. By inspecting the n_f -dependence of the fixed-order corrections to the electromagnetic decay rates $\Gamma_{\eta_c \rightarrow \gamma\gamma}$ and $\Gamma_{J/\psi \rightarrow e^+e^-}$, which are available up to two [9,15,16] and three loops [31–35], respectively, we find that the fixed-order corrections are also significant beyond the large n_f limit in those electromagnetic decay rates. Hence, the bubble-chain resummation calculations of those decay rates in Ref. [36] seem to fail to reproduce the fixed-order calculations.

We have examined a method that is often employed for computing renormalon singularities in the heavy-quark pole mass described in Refs. [37,38], where the renormalon ambiguities that scale like powers of Λ_{QCD} are subtracted from the divergent perturbation series. This method has an advantage that it does not rely on the large- n_f limit. We have found that a naïve application of the method in Refs. [37,38] to the electromagnetic decay rates $\Gamma_{\eta_c \rightarrow \gamma\gamma}$, $\Gamma_{J/\psi \rightarrow e^+e^-}$ and the inclusive decay rate of η_c lead to estimates of the perturbative series that are in poor agreement with the fixed-order corrections.

By combining the resummed result for R and the fixed-order calculations valid up to next-to-next-to-leading order in α_s , we have obtained precise predictions of R for the decay of η_b with uncertainties that could be as small as 5%. Therefore, the measurement of $\Gamma_{\eta_b \rightarrow \gamma\gamma}$ in ongoing and future experiments is highly anticipated. We also look forward to improved experimental measurements for the decay rate of η_b , as well as the total and partial decay rates of η_c .

ACKNOWLEDGMENTS

We thank Antonio Vairo for his collaboration on this project, his valuable comments and careful reading of the manuscript. The work of N. B. is supported by the DFG and the NSFC through funds provided to the Sino-German CRC 110 ‘‘Symmetries and the Emergence of Structure in QCD’’ (NSFC Grant No. 11621131001). N. B. also acknowledges support from the DFG cluster of excellence ‘‘Origin and structure of the universe’’ (www.universe-cluster.de). This work was supported in part by the German Excellence Initiative and the European Union Seventh Framework Program under Grant Agreement No. 291763 as well as the European Union’s Marie Curie COFUND program (J. K.). The work of H. S. C. is supported by the Alexander von Humboldt Foundation. The work of H. S. C. is also supported by the DFG cluster of excellence ‘‘Origin and Structure of the Universe’’ (www.universe-cluster.de).

APPENDIX: COMPUTATION OF $T(t, \tau)$

In this Appendix, we calculate $T(t, \tau)$ defined in Eq. (22),

$$T(t, \tau) = \frac{1}{\pi^2} \int_0^1 \int_0^1 dx dy \text{Im} \left[\frac{x^{-t} e^{i\pi t}}{x + i\varepsilon} \right] \text{Im} \left[\frac{y^{-\tau} e^{i\pi \tau}}{y + i\varepsilon} \right] \times f(x, y) \theta(1 - \sqrt{x} - \sqrt{y}),$$

with $f(x, y)$ given in Eq. (19). We need to calculate the derivatives of $T(t, \tau)$ at $t = \tau = 0$. As infrared regulators we assume $\tau < 0$ and $t < 0$ so that the integral over x and y become finite. We then drop the small $i\varepsilon$ terms, and we write T as

$$T(t, \tau) = \frac{1}{\pi^2} \sin(\pi t) \sin(\pi \tau) \int_0^1 \int_0^1 dx dy x^{-t-1} y^{-\tau-1} f(x, y) \times \theta(1 - \sqrt{x} - \sqrt{y}). \quad (\text{A1})$$

Using change of variables $y = (1 - \sqrt{x})^2 z$, we obtain

$$T(t, \tau) = \frac{1}{\pi^2} \sin(\pi t) \sin(\pi \tau) \int_0^1 \int_0^1 dx dz x^{-t-1} z^{-\tau-1} \times (1 - \sqrt{x})^{-2\tau} f(x, (1 - \sqrt{x})^2 z). \quad (\text{A2})$$

Let us now focus on $f(x, y)$, which can be written as

$$\begin{aligned} f(x, y) &= \frac{[(1 - \sqrt{x})^2 - y][(1 + \sqrt{x})^2 - y]}{(1 - x - y)^2}]^{3/2} \\ &= (1 - x)(1 - z)^{3/2} \frac{(1 - \xi^2 z)^{3/2}}{(1 - \xi z)^2} \\ &= (1 - x)(1 - z)^{3/2} \sum_{j,k=0}^{\infty} C_{jk} \xi^{2k+j} z^{k+j}, \end{aligned} \quad (\text{A3})$$

where

$$\xi = \frac{1 - \sqrt{x}}{1 + \sqrt{x}}, \quad (\text{A4})$$

$$C_{jk} = (j + 1) \frac{\Gamma(k - 3/2)}{\Gamma(-3/2)\Gamma(k + 1)}. \quad (\text{A5})$$

Plugging Eq. (A3) in Eq. (A2) we obtain

$$\begin{aligned} T(t, \tau) &= \frac{1}{\pi^2} \sin(\pi t) \sin(\pi \tau) \sum_{j,k=0}^{\infty} C_{jk} \int_0^1 dz z^{k+j-\tau-1} (1 - z)^{3/2} \\ &\quad \times \int_0^1 dx x^{-t-1} (1 - x)(1 - \sqrt{x})^{-2\tau} \xi^{2k+j} \\ &= \frac{1}{\pi^2} \sin(\pi t) \sin(\pi \tau) \sum_{j,k=0}^{\infty} C_{jk} B\left(\frac{5}{2}, k + j - \tau\right) \\ &\quad \times \int_0^1 dx x^{-t-1} (1 - x)(1 - \sqrt{x})^{-2\tau} \xi^{2k+j} \\ &= \frac{2}{\pi^2} \sin(\pi t) \sin(\pi \tau) \sum_{j,k=0}^{\infty} C_{jk} B\left(\frac{5}{2}, k + j - \tau\right) \\ &\quad \times \int_0^1 dX X^{-2t-1} (1 - X)^{2k+j+1-2\tau} (1 + X)^{1-2k-j} \\ &= \frac{2}{\pi^2} \sin(\pi t) \sin(\pi \tau) \sum_{j,k=0}^{\infty} C_{jk} B\left(\frac{5}{2}, k + j - \tau\right) \\ &\quad \times B(-2t, 2k + j + 2 - 2\tau) \\ &\quad \times F(2k + j - 1, -2t; 2k + j + 2 - 2\tau - 2t; -1), \end{aligned} \quad (\text{A6})$$

with the hypergeometric function

$$F(\alpha, \beta; \gamma; z) = \frac{1}{B(\beta, \gamma - \beta)} \int_0^1 dx x^{\beta-1} (1 - x)^{\gamma-\beta-1} \times (1 - zx)^{-\alpha}. \quad (\text{A7})$$

Using the identities

$$F(\alpha, \beta; \gamma; z) = F(\beta, \alpha; \gamma; z), \quad (\text{A8})$$

$$F(\alpha, \beta; \gamma; -1) = 2^{-\alpha} F\left(\alpha, \gamma - \beta; \gamma; \frac{1}{2}\right), \quad (\text{A9})$$

we replace

$$F(2k + j - 1, -2t; 2k + j + 2 - 2\tau - 2t; -1) \rightarrow 2^{2t} \\ \times F\left(-2t, 3 - 2t - 2\tau; 2k + j + 2 - 2\tau - 2t; \frac{1}{2}\right);$$

Eq. (A6) reads

$$T(t, \tau) = \frac{2}{\pi^2} \sin(\pi t) \sin(\pi \tau) \Gamma(-2t) 2^{2t} \sum_{j,k=0}^{\infty} (j+1) \\ \times \frac{\Gamma(k-3/2)}{\Gamma(-3/2)\Gamma(k+1)} \frac{\Gamma(5/2)\Gamma(k+j-\tau)}{\Gamma(5/2+k+j-\tau)} \\ \times \frac{\Gamma(2k+j+2-2\tau)}{\Gamma(2k+j+2-2\tau-2t)} \\ \times F\left(-2t, 3-2t-2\tau; 2k+j+2-2\tau-2t; \frac{1}{2}\right). \quad (\text{A10})$$

Using Legendre's duplication formula and Euler's reflection formula,

$$\Gamma(-2t) = \frac{2^{-2t}\Gamma(-t)\Gamma(1/2-t)}{2\Gamma(1/2)}, \quad (\text{A11})$$

$$\sin(\pi t) = \frac{-\pi}{\Gamma(1+t)\Gamma(-t)}, \quad (\text{A12})$$

we now write Eq. (A10) as

$$T(t, \tau) = \frac{1}{\Gamma(1+t)\Gamma(1+\tau)} \frac{\Gamma(1/2-t)}{\Gamma(1/2)\Gamma(-\tau)} \sum_{j,k=0}^{\infty} (j+1) \\ \times \frac{\Gamma(k-3/2)}{\Gamma(-3/2)\Gamma(k+1)} \frac{\Gamma(5/2)\Gamma(k+j-\tau)}{\Gamma(5/2+k+j-\tau)} \\ \times \frac{\Gamma(2k+j+2-2\tau)}{\Gamma(2k+j+2-2\tau-2t)} \\ \times F\left(-2t, 3-2t-2\tau; 2k+j+2-2\tau-2t; \frac{1}{2}\right). \quad (\text{A13})$$

Note that we have

$$T(t, 0) = T(0, t) = \frac{\sin(\pi t)}{\pi t(1-t)}. \quad (\text{A14})$$

This relation immediately yields $T(0, 0) = 1$.

The expression given in Eq. (A13) contains summations over j and k . Now we discuss how to improve the radius of convergences of the sums by adding and subtracting some terms that can be summed up analytically. First, instead of using Eq. (A3), we expand f as

$$f(x, y) = (1-x)(1-z)^{3/2} \\ \times \left\{ \sum_{j,k=0}^{\infty} C_{jk} [z^{k+j} \xi^{2k+j} - f_0 - f_1 (z\xi)^{k+j}] \right. \\ \left. + f_0 (1-z)^{-1/2} + f_1 \sum_{l=0}^{\infty} \frac{\Gamma(l+\frac{1}{2})}{\Gamma(\frac{1}{2})\Gamma(l+1)} (z\xi)^l \right\}, \quad (\text{A15})$$

where f_0 and f_1 can be any constants or any functions of t and τ that are analytic in the vicinity of the origin of the complex- t and complex- τ planes. Then, we write Eq. (A13) as

$$T(t, \tau) = T_0(t, \tau) + T_1(t, \tau) + T_2(t, \tau), \quad (\text{A16})$$

where

$$T_0(t, \tau) \equiv f_0 \frac{-\tau}{\Gamma(1+t)\Gamma(1+\tau)} \frac{\Gamma(\frac{7}{2})}{\Gamma(\frac{3}{2})} \frac{\Gamma(\frac{3}{2}-t)}{\Gamma(\frac{7}{2}-2t)} \frac{\Gamma(2-2t)}{\Gamma(3-\tau-2t)} \quad (\text{A17})$$

$$T_1(t, \tau) \equiv \frac{1}{\Gamma(1+t)\Gamma(1+\tau)} \frac{\Gamma(\frac{1}{2}-t)}{\Gamma(\frac{1}{2})\Gamma(-\tau)} \sum_{l=0}^{\infty} \\ \times \frac{\Gamma(l+\frac{1}{2})}{\Gamma(\frac{1}{2})\Gamma(l+1)} \frac{\Gamma(\frac{5}{2})\Gamma(l-\tau)}{\Gamma(\frac{5}{2}+l-\tau)} \\ \times \left\{ f_1 \frac{\Gamma(l+2-2\tau)}{\Gamma(l+2-2\tau-2t)} \right. \\ \times F\left(-2t, 3-2t-2\tau; l+2-2\tau-2t; \frac{1}{2}\right) \\ \left. - f_0 \frac{(l-\tau)\Gamma(\frac{5}{2}+l-\tau)}{\Gamma(\frac{7}{2}+l-\tau-2t)} \right\} \quad (\text{A18})$$

$$T_2(t, \tau) \equiv \frac{1}{\Gamma(1+t)\Gamma(1+\tau)} \frac{\Gamma(\frac{1}{2}-t)}{\Gamma(\frac{1}{2})\Gamma(-\tau)} \sum_{j,k=0}^{\infty} (j+1) \frac{\Gamma(k-\frac{3}{2})}{\Gamma(-\frac{3}{2})\Gamma(k+1)} \frac{\Gamma(\frac{5}{2})\Gamma(k+j-\tau)}{\Gamma(\frac{5}{2}+k+j-\tau)} \\ \times \left\{ \frac{\Gamma(2k+j+2-2\tau)}{\Gamma(2k+j+2-2\tau-2t)} F\left(-2t, 3-2t-2\tau; 2k+j+2-2\tau-2t; \frac{1}{2}\right) \right. \\ - f_1 \frac{\Gamma(k+j+2-2\tau)}{\Gamma(k+j+2-2\tau-2t)} F\left(-2t, 3-2t-2\tau; k+j+2-2\tau-2t; \frac{1}{2}\right) \\ \left. - f_0 \frac{2tk\Gamma(\frac{5}{2}+k+j-\tau)}{\Gamma(\frac{7}{2}+k+j-\tau-2t)} \right\}. \quad (\text{A19})$$

Setting f_0 and f_1 to unity, the above expression for $T(t, \tau)$ is convergent for all $t < 1$. In particular, one can verify that $T(t, \tau)$ does not have any singularity at $t = \frac{1}{2}$ although it contains a factor of $\Gamma(t - 1/2)$. One can also show that

$$\lim_{\tau \rightarrow 1} (1 - \tau)T(t, \tau) = -\frac{3}{\pi} \sin(\pi t), \quad (\text{A20})$$

and by symmetry argument

$$\lim_{t \rightarrow 1} (1 - t)T(t, \tau) = -\frac{3}{\pi} \sin(\pi \tau). \quad (\text{A21})$$

-
- [1] A. J. Bevan *et al.* (BABAR and Belle Collaborations), *Eur. Phys. J. C* **74**, 3026 (2014).
- [2] G. T. Bodwin, E. Braaten, and G. P. Lepage, *Phys. Rev. D* **51**, 1125 (1995); **55**, 5853(E) (1997).
- [3] G. T. Bodwin and A. Petrelli, *Phys. Rev. D* **66**, 094011 (2002); **87**, 039902(E) (2013).
- [4] N. Brambilla, E. Mereghetti, and A. Vairo, *Phys. Rev. D* **79**, 074002 (2009); **83**, 079904(E) (2011).
- [5] G. T. Bodwin and Y. Q. Chen, *Phys. Rev. D* **64**, 114008 (2001).
- [6] C. Patrignani *et al.* (Particle Data Group), *Chin. Phys. C* **40**, 100001 (2016).
- [7] N. Brambilla, D. Eiras, A. Pineda, J. Soto, and A. Vairo, *Phys. Rev. Lett.* **88**, 012003 (2001).
- [8] N. Brambilla, D. Eiras, A. Pineda, J. Soto, and A. Vairo, *Phys. Rev. D* **67**, 034018 (2003).
- [9] R. Barbieri, E. d'Emilio, G. Curci, and E. Remiddi, *Nucl. Phys.* **B154**, 535 (1979).
- [10] K. Hagiwara, C. B. Kim, and T. Yoshino, *Nucl. Phys.* **B177**, 461 (1981).
- [11] F. Feng, Y. Jia, and W. L. Sang, *Phys. Rev. Lett.* **119**, 252001 (2017).
- [12] W. Y. Keung and I. J. Muzinich, *Phys. Rev. D* **27**, 1518 (1983).
- [13] H. K. Guo, Y. Q. Ma, and K. T. Chao, *Phys. Rev. D* **83**, 114038 (2011).
- [14] A. Petrelli, M. Cacciari, M. Greco, F. Maltoni, and M. L. Mangano, *Nucl. Phys.* **B514**, 245 (1998).
- [15] A. Czarnecki and K. Melnikov, *Phys. Lett. B* **519**, 212 (2001).
- [16] F. Feng, Y. Jia, and W. L. Sang, *Phys. Rev. Lett.* **115**, 222001 (2015).
- [17] Y. Jia, X. T. Yang, W. L. Sang, and J. Xu, *J. High Energy Phys.* **06** (2011) 097.
- [18] D. J. Gross and A. Neveu, *Phys. Rev. D* **10**, 3235 (1974).
- [19] B. E. Lautrup, *Phys. Lett.* **69B**, 109 (1977).
- [20] G. 't Hooft, in *The Whys of Subnuclear Physics*, edited by A. Zichichi (Plenum, New York, 1978).
- [21] G. T. Bodwin and Y. Q. Chen, *Phys. Rev. D* **60**, 054008 (1999).
- [22] M. Beneke and V. M. Braun, *Phys. Lett. B* **348**, 513 (1995).
- [23] B. S. DeWitt, *Phys. Rev.* **162**, 1195 (1967).
- [24] J. H. Kuhn, J. Kaplan, and E. G. O. Safiani, *Nucl. Phys.* **B157**, 125 (1979).
- [25] B. Guberina, J. H. Kuhn, R. D. Peccei, and R. Ruckl, *Nucl. Phys.* **B174**, 317 (1980).
- [26] K. G. Chetyrkin, J. H. Kuhn, and M. Steinhauser, *Comput. Phys. Commun.* **133**, 43 (2000).
- [27] H. S. Chung, J. Lee, and C. Yu, *Phys. Lett. B* **697**, 48 (2011).
- [28] Y. Kiyo, A. Pineda, and A. Signer, *Nucl. Phys.* **B841**, 231 (2010).
- [29] B. L. Du, X. G. Wu, J. Zeng, S. Bu, and J. M. Shen, *Eur. Phys. J. C* **78**, 61 (2018).
- [30] A. L. Kataev and S. V. Mikhailov, *Phys. Rev. D* **91**, 014007 (2015).
- [31] R. Barbieri, R. Gatto, R. Kogerler, and Z. Kunszt, *Phys. Lett.* **57B**, 455 (1975).
- [32] W. Celmaster, *Phys. Rev. D* **19**, 1517 (1979).
- [33] M. Beneke, A. Signer, and V. A. Smirnov, *Phys. Rev. Lett.* **80**, 2535 (1998).
- [34] A. Czarnecki and K. Melnikov, *Phys. Rev. Lett.* **80**, 2531 (1998).
- [35] P. Marquard, J. H. Piclum, D. Seidel, and M. Steinhauser, *Phys. Rev. D* **89**, 034027 (2014).
- [36] E. Braaten and Y. Q. Chen, *Phys. Rev. D* **57**, 4236 (1998); **59**, 079901(E) (1999).
- [37] A. Pineda, *J. High Energy Phys.* **06** (2001) 022.
- [38] J. Komijani, *J. High Energy Phys.* **08** (2017) 062.